SOVIET PHYSICS USPEKHI VOLUME 13, NUMBER 6 MAY-JUNE 1971

539.30/.32

NONLINEAR PHENOMENA IN THE PROPAGATION OF ELASTIC WAVES IN SOLIDS*

L. K. ZAREMBO and V. A. KRASIL'NIKOV

Moscow State University

Usp. Fiz. Nauk 102, 549–586 (December, 1970)

I. INTRODUCTION

IT is well known that under sufficiently strong stresses solids go over into plastic flow, harden, etc. The nonlinear dependence of the strain on the stress at large stresses ($\gtrsim 10^2$–10^3 kg/cm^2), where the deformation is already inelastic, is of no interest to us. When ultrasonic or hypersonic waves propagate, the amplitude of the stresses usually does not exceed several kg/cm^2, and the deformation can be regarded as fully elastic. However, as shown by results of numerical experiments, under these conditions there are clearly pronounced nonlinear effects such as generation of acoustic harmonics, Raman scattering of sound by sound, nonlinear acoustic resonance, and many others, which are dealt with in the present article. According to the nonlinear theory of elasticity, macroscopic nonlinear elastic properties of solids are determined, on the one hand, by the nonlinear connection between the components of the strain tensor and the derivatives of the displacements with respect to the coordinates. This feature of finite strains does not depend on the physical properties of the deformed body and is usually called geometrical nonlinearity. The physical nonlinearity is the consequence of the fact that the internal energy of the deformed solid is not only a quadratic function of the invariants of the strain tensor, but also a cubic one etc. The physical nonlinearity is determined by the elastic moduli of third, fourth, and higher orders†. The existence of both geometrical and physical nonlinearity makes the generalized Hooke's law (the connection between the stresses and the strains) also nonlinear, and its nonlinearities are determined, generally speaking, by the geometrical and physical nonlinearities simultaneously. Such a phenomenological model of a nonlinear solid, however, is not quite complete. It is shown by the experimental results, in particular, that even in solids with the simplest structure and properties (isotropic dielectrics) the magnitude of the aforementioned nonlinear acoustic effects depends on the residual internal stresses, and in crystals it depends on the dislocations. These features of real solids lead to nonlinear interactions that are forbidden by the theory of elasticity of a homogeneous isotropic body. The nonlinear acoustic effects become even more complicated when the solid is such that there is a sufficiently strong coupling between the elastic oscillations and excitations of another type, for example in piezo- or ferroelectrics or in ferromagnets and ferrodielectrics. In these solids, one can observe "on the acoustic side" not only the aforementioned effects, but also nonlinear effects connected with the nonlinearity of the piezoeffect and of the magnetostriction effect (the nonlinear dependence of the mechanical displacements on the electromagnetic field intensity). These properties can be phenomenologically accounted for in the internal energy.

We have discussed above the macroscopic nonlinearity of solids. The microscopic nonlinearity, naturally, is determined by the nonlinearity of the interatomic forces. The potential energy of the atom in the field of all the remaining atoms of the crystal can be expanded in a series about the equilibrium position of the atom; besides the quadratic terms, this expansion contains terms proportional to the cube, fourth power, etc. The latter determine the nonlinear (sometimes called anharmonic) character of the interatomic forces. Frequently this nonlinearity is called the lattice nonlinearity. The lattice nonlinearity is responsible for a number of macroscopic well-investigated phenomena, such as the thermal expansion of solids (the change of the average interatomic distance with change in temperature), the deviation from the law of Dulong and Petit for the specific heat of a solid at high temperatures. Thermal vibrations of atoms about the equilibrium position can be represented as a superposition of plane waves of different frequencies and with different wave vectors, the so-called thermal phonons. In the approximation of linear interatomic forces, the phonons do not interact with one another. The anharmonic character of the interatomic forces leads to a possible "production" of a new phonon (or phonons) as a result of the interaction of two (or more) phonons. The phonon-phonon interactions play an important role in the explanation of a large number of kinetic phenomena in solids, such as the thermal conductivity of solids and the absorption of sound. Phonon-phonon interactions are a part of a more general problem of the interaction of quasiparticles or elementary excitations in solids. Great importance is being attached of late to investigations of the interaction of phonons with phonons, electrons, photons, and magnons, and intensive research is going on in these fields.

The concept of the phonon as a quantum of lattice oscillations pertained at first to very high oscillation frequencies, where one could not ignore the discreteness of the crystal-lattice structure. At the present time it can be stated that, with the exception of singularities determined by the discrete structure of the lattice, the interaction of elastic waves at hypersonic or even ultrasonic frequencies obeys the same selection rules as the phonon-phonon interactions. This explains why the term "phonon-phonon interaction" is now used not only for thermal phonons, but also for

*Expanded version of a paper delivered at the scientific session of the Division of General Physics and Astronomy of the USSR Academy of Sciences on 16 January 1969.

†In accordance with the universally accepted terminology, the elastic moduli in the linear Hooke's law (where the internal energy of the deformed solid is a quadratic function of the invariants of the strain tensor) are called elastic moduli of second order.

nonlinear interactions of artificially excited low-frequency elastic waves ("coherent" phonons).

Phonon-phonon interaction was experimentally observed relatively recently in the propagation of "coherent" phonons of low energies—elastic waves at ultrasonic frequencies[1,2]. The amplitude of the sound pressure at which nonlinear distortion of the sinusoidal elastic wave or generation of harmonics is clearly observed does not exceed several atmospheres and lies in the region which quite recently was still regarded as belonging to linear acoustics. An investigation of these effects makes it possible, on the one hand, to obtain information on nonlinear elastic properties of solids, and on the other hand, to "stimulate" phonon-phonon interaction processes with coherent phonons. These investigations yield much useful information for a more detailed understanding of many kinetic processes in solids. In addition, different nonlinear effects can ultimately have certain practical applications.

In liquids, the nonlinear effects occurring during the propagation of elastic waves have by now been sufficiently well investigated[3]. In isotropic solids, owing to the possibility of propagation of both longitudinal and transverse waves, the number of permissible nonlinear interactions is much larger than in liquids, where plane waves interact only when they propagate in the same directions. Even more varied and complicated is the nonlinear interaction of waves in crystals; in this field there is still no more or less satisfactory theory. The low efficiency of nonlinear conversion in all the investigated solids limits the possibility of practical application of different acoustic nonlinear effects. At the present time, incidentally, there are known solids—piezosemiconductors—in which, owing to the electron-phonon interaction, the effective elastic nonlinearity is comparable in order of magnitude with the nonlinearity of liquids, giving grounds for hoping to use nonlinear phenomena in these solids for different practical purposes in the future. Certain prospects of practical utilization of nonlinear phenomena are apparently uncovered in the case of surface Rayleigh waves, where the nonlinear effects are sufficiently strongly pronounced. Observation of harmonic generation and of nonlinear wave interaction uncovers additional possibilities of measuring the elastic moduli of third order and, in final analysis, the anharmonicity of the lattice. A comparison of the experimental results with the theoretical model results yields additional information on the character of the forces of interatomic interaction, in analogy with such parameters as the equilibrium dimension of the crystal cell and the second-order elastic moduli.

II. ELEMENTS OF NONLINEAR THEORY OF ELASTICITY

We shall need in what follows certain results of the nonlinear theory of elasticity. Let us stop to discuss this theory briefly. (for details see[4-7]).

1. Strains. The exact expression for the components of the strain tensor* is

$$u_{ij}=\frac{1}{2}\left(\frac{\partial u_i}{\partial x_j}+\frac{\partial u_j}{\partial x_i}+\frac{\partial u_l}{\partial x_i}\frac{\partial u_l}{\partial x_j}\right)\eta_s, \tag{1}$$

*Repeated indices denote summation throughout this article.

where u_i are the components of the displacement vector, i, j = 1, 2, 3; s = 1, 2, ..., 6, and the realized transition from i, j to s is the one customarily used in crystallography: 11 → 1, 22 → 2, 33 → 3, 23 = 32 → 4, 13 = 31 → 5, and 12 = 21 → 6. The invariants of the strain tensor are

$$\left.\begin{aligned} I_1&=u_{ll}=\eta_1+\eta_2+\eta_3,\\ I_2&=\frac{1}{2}(u_{ll}^2-u_{ik}^2)=\eta_1\eta_2+\eta_1\eta_3+\eta_2\eta_3-(\eta_4^2+\eta_5^2+\eta_6^2),\\ I_3&=\det|u_{ik}|=\frac{1}{3}\left(u_{ik}u_{il}u_{kl}-\frac{3}{2}u_{ik}^2u_{ll}-\frac{1}{2}u_{ll}^3\right)\\ &=\eta_1\eta_2\eta_3+2\eta_4\eta_5\eta_6-(\eta_1\eta_4^2+\eta_2\eta_5^2+\eta_3\eta_6^2). \end{aligned}\right\} \tag{2}$$

2. Internal energy and third-order moduli. The internal energy of a deformed isotropic body should not depend on the choice of the coordinate system. It is invariant against rotation and displacement of the deformed body as a unit. This is possible only in the case when the internal energy is a function of the invariants of the strain tensor U = U(I_1, I_2, I_3, S), where S is the entropy. Since the strains, and consequently also the invariants, are small, U can be expanded in a series about the undeformed state. The undeformed state will henceforth be considered to be in equilibrium and $\partial U/\partial I_1|_0 = 0$. Therefore the expansion begins with the quadratic terms. The second-order moduli are defined as the coefficients preceding the terms of second order of smallness:

$$\mu=-\frac{1}{2}\frac{\partial U}{\partial I_2}\Big|_0, \quad K+\frac{4}{3}\mu=\frac{\partial^2 U}{\partial I_1^2}\Big|_0, \tag{3}$$

where μ is the shear modulus and K the bulk modulus. The coefficients preceding the quantities of third order of smallness give the third-order moduli:

$$\left.\begin{aligned} &\frac{\partial U}{\partial I_3}\Big|_0=n=A, \quad \frac{\partial^2 U}{\partial I_1\partial I_2}=-4m=-2A-4B,\\ &\frac{\partial^3 U}{\partial I_1^3}\Big|_0=4m+2l=2A+6B+2C, \end{aligned}\right\} \tag{4}$$

where n, l, and m are Murnaghan's third-order moduli. A, B, and C are the Landau third-order moduli. The next approximation would require the introduction of four fourth-order moduli, five fifth-order moduli, etc. We shall henceforth confine ourselves to the second approximation only (we retain only terms of third order of smallness in the expansion of the internal energy), and consequently to the five-constant elasticity theory. The third-order moduli of certain solids are given in Table I.

The situation is more complicated with crystals, where the internal energy is invariant only against the transformations characteristic of each crystal class. In the general case, the internal energy U of a crystal is a polynomial of the strain-tensor components

$$U=\frac{1}{2}c_{ijpq}u_{ij}u_{pq}+\frac{1}{6}C_{ijpqrs}u_{ij}u_{pq}u_{rs}, \tag{5}$$

where C_{ijpq} and C_{ijpqrs} are the elastic moduli of second and third order, respectively. This is the definition of third-order moduli after[13]. It is obvious that $C_{ijklmn} = C_{klijm} = C_{mnijkl} = C_{ijmnkl} = C_{klmnij} = C_{mnklij}$. In analogy with the procedure in linear elasticity theory, we can introduce abbreviated symbols for the third-order moduli, by changing over from two indices to one using the rules mentioned above. The third-order moduli of certain crystals are given in

Table II. Cubic crystals of the most symmetrical subgroups O, O^h, and T^d have six independent third-order moduli, those of the subgroups T and T^h have eight independent moduli. The independent third-order moduli of different crystal classes are listed in Table III. In the general case, an anisotropic solid has a total of 216 third-order moduli. From the symmetry conditions, however, one can obtain additional connections between the third-order moduli. For a crystal with the lowest symmetry of triclinic class, the number of third-order moduli decreases to 56. The number of moduli of order higher than the third increases rapidly with increasing order. For example, a triclinic crystal has 126 fourth-order and 352 fifth-order moduli.

As seen from the data of Tables I and II, most presently-known third-order moduli were determined from measurements of the dependence of the velocity of the elastic waves on the static pressure, i.e., according to[13] these are mixed (isothermal-adiabatic) moduli. Acoustic methods of measuring different nonlinear effects, as will be shown below, make it possible in principle to determine the adiabatic third-order moduli.

Table I. Third-order elastic moduli of certain solids ($\times 10^{-11}$ n/m^2)

Material	Reference	Murnaghan's moduli			Landau's moduli			Remark*
		l	m	n	A	B	C	
Polystyrene	8	−0.19±0.03	−0.13±0.03	−0.1±0.01	−0.1±0.01	−0.08±0.04	−0.11±0.07	M^{ST}
"Armco" iron	8	−0.35±0.07	−10.3±0.7	11±11	11±11	−15.8±6.2	12.3±6.9	M^{ST}
Nickel steel 535	9	−0.46	−5.9	−7.3	−7.3	−2.3	−1.8	M^{ST}
Steel C1018	10	—	—	−5.7±0.3	−5.7±0.3	—	—	M^S
Steel 60 C2H2A	11	−3.4	−6.3	−7.6	−7.6	−2.5	−0.9	M^{ST}
« «	12	—	—	−7.6	−7.6	—	—	M^{ST}
Aluminum 6016-T6	10	—	—	−3.1±0.1	−3.1±0.1	—	—	M^S
Aluminum 1100-F	10	—	—	−4.8±0.4	−4.8±0.4	—	—	M^S
Fused quartz	10	—	—	−2.3±0.1	−2.3±0.1	—	—	M^S
Glass (pyrex)	8	0.14±0.4	0.9±0.5	4.2±3.5	4.2±3.5	−1.18±2.35	−1.32±2.6	M^{ST}

*The table lists both the adiabatic moduli, designated M^S, and mixed moduli M^{ST} (see below concerning methods of measuring third-order moduli).

Table II. Third-order elastic moduli of crystals ($\times 10^{-12}$ dyne/cm^2) (in Bragger's notation)

Crystal	Reference	c_{111}	c_{112}	c_{123}	c_{456}	c_{144}	c_{166}	c_{155}	Remark
NaCl	2	−8.7	—	—	—	—	—	—	C^S
	15	−6.42	—	—	—	—	—	—	C^S
	16	−8.80	−0.57	0.28	0.27±0.01	0.26±0.01	−0.61±0.01	—	C^{ST}
	17	−8.60	−0.52	0.16	0.25	0.26	−0.57	—	C^{ST}
	18	−5.45	−0.69	0.27	0.33	0.33	−0.63	—	Theoretical
	19	−8.64±0.08	−0.50±0.04	0.09±0.08	0.13±0.02	0.07±0.03	−0.59±0.01	—	C^{TS}
	20	−8.3±0.8	—	—	—	—	—	—	C^S
	21	−8.43±0.33	−0.50±0.07	0.46±0.09	0.26±0.01	0.29±0.05	−0.60±0.04	—	C^{TS}
	22	−8.23±0.20	0.02±0.50	0.53±0.07	0.20±0.01	0.23±0.03	−0.61±0.03	—	C^{TS}
NaF	18	−7.14	−1.44	0.658	0.76	0.76	−1.28	—	Theoretical
KBr	18	−4.64	−0.39	0.111	0.186	0.186	−0.33	—	Theoretical
KCl	16	−7.01	−0.224	0.133	0.118	0.127	−0.245	—	C^{TS}
	20	−7.1±0.7	—	—	—	—	—	—	C^S
	21	−7.26±0.39	−0.24±0.04	0.11±0.04	0.16±0.01	0.23±0.04	−0.26±0.02	—	C^{TS}
	18	−5.07	−0.458	0.148	0.207	0.207	−0.40	—	Theoretical
KJ	18	−4.71	−0.314	0.074	0.145	0.145	−0.26	—	Theoretical
BaF_2	30	−5.84±0.15	−2.99±0.14	−2.06±0.11	−0.271±0.001	−1.21±0.03	−0.889±0.019	—	C^{TS}
LiF	18	−20.7	−2.56	1.11	1.32	1.32	−2.42	—	Theoretical
	21	−14.23±0.30	−2.64±0.28	1.56±0.28	0.94±0.06	−0.85±0.10	−2.73±0.13	—	C^{TS}
Ge	31	−7.16±0.2	−4.03±0.1	−0.18±0.3	−0.47±0.1	−0.53±0.5	−3.15±0.05	—	C^{TS}
	32	−6.96±1.08	−3.40±0.62	+0.25±0.43	−0.42±0.06	+0.18±0.21	−2.96±0.22	—	C^{TS}
	23	—	−2.9±0.3	−0.22±0.2	−0.41±0.05	−0.08±0.09	−3.03±0.09	—	C^{TS}
	24	−7.10±0.06	−3.89±0.03	−0.18±0.06	−0.53±0.07	−0.23±0.16	−2.92±0.08	—	C^{TS}
	26	$\frac{1}{6}C^S_{111}+C^S_{112}+2C^S_{144}+4C^S_{166}+\frac{1}{3}C^S_{123}+\frac{8}{3}C^S_{456}=18{,}69$							

Table II (Continued)

Crystal	Reference	c_{111}	c_{112}	c_{123}	c_{456}	c_{144}	c_{166}	c_{155}	Remark
Si	24	−8.25±0.10	−4.51±0.05	−0.64±0.10	−0.64±0.20	0.12±0.25	−3.10±0.10	—	C^{TS}
	26	$\frac{1}{6}C^S_{111}+C^S_{112}+2C^S_{144}+4C^S_{166}+\frac{1}{3}C^S_{123}+\frac{8}{3}C^S_{456}=19.86$							
InSb	25	−3.14±0.2	−2.10±0.2	−0.48±0.1	0.002±0.01	0.09±0.1	−1.18±0.1	—	C^{TS}
Cu	27	−15.0±1.5	−8.5±1.0	−2.5±1.0	−0.16±0.1	−1.35±0.15	−6.45±0.1	—	C^{TS} at $T=295°$ K
	27	−19.5±2.0	−11.5±1.5	−4.2±1.5	+0.12±0.1	−1.25±0.25	−7.25±0.3	—	C^{TS} at $T=77°$ K
	27	−20.0±2.0	−12.2±1.5	−5.0±1.5	0.25±0.08	−1.32±0.2	−7.05±0.25	—	C^{TS} at $T=4,2°$ K
	26	$\frac{1}{6}C^S_{111}+C^S_{112}+2C^S_{144}+4C^S_{166}+\frac{1}{3}C^S_{123}+\frac{8}{3}C^S_{456}=27,6$							
	29 *)	−14.27±1.4	−7.78±0.8	−2.65±1.5	1.17±1.6	−0.06±2.3	−7.71±1.1	—	
	29 *)	−14.27±1.4	−8.87±0.8	−1.77±1.5	0.66±1.6	−0.63±2.3	−7.44±1.1	—	
	33	−12.71±0.22	−8.14±0.09	−0.50±0.18	−0.95±0.87	−0.03±0.09	−7.80±0.05	—	C^{TS}
Ag	33	−8.43±0.37	−5.29±0.18	1.89±0.37	+0.83±0.08	0.56±0.26	−6.37±0.13	—	C^{TS}
Au	33	−17.29±0.21	−9.22±0.12	−2.33±0.49	−0.12±0.16	−0.13±0.32	−6.48±0.17	—	C^{TS}
MgO	31	−48.95±1.5	−0.95±0.9	−0.69±2.2	1.47±0.1	1.13±0.4	−6.59±0.2	—	C^{TS}
$Y_3Fe_5O_{12}$ (YIG)	28	−23.3±0.8	−7.17±0.6	−0.33±1.3	−0.97±0.16	−1.48±0.29	—	−3.06±0.14	C^{TS}
SiO_2 (quartz)	34	−2.10	−3.45	−2.94	—	−1.34	—	−2.0	C^{TS}
		$C_{113}=+0.12$, $C_{114}=-1.63$, $C_{124}=-0.15$, $C_{133}=-3.12$, $C_{134}=+0.02$, $C_{222}=-3.32$, $C_{333}=-8.15$, $C_{344}=-1.10$, $C_{444}=-2.76$							

*Three combinations of adiabatic moduli are determined, and the results of measurement of the mixed moduli C^{TS}_{ijk} in [33] (first line) and in [27] (second line) were used to calculate all six moduli.

Table III. Independent elastic third-order moduli of crystals

Class	Independent moduli
Cubic { O, O^h, T^h / T, T^h	$C_{111}, C_{112}, C_{123}, C_{456}, C_{144}, C_{166}$ / $C_{111}, C_{112}, C_{123}, C_{456}, C_{144}, C_{166}, C_{113}, C_{155}$
Hexagonal	$C_{111}, C_{112}, C_{113}, C_{133}, C_{333}, C_{123}, C_{144}, C_{166}$ $C_{344}, C_{155}, C_{366}, C_{456}$
Tetragonal	$C_{111}, C_{112}, C_{113}, C_{114}, C_{123}, C_{124}, C_{144}, C_{133}$ $C_{134}, C_{155}, C_{222}, C_{333}, C_{344}$
Trigonal	$C_{111}, C_{112}, C_{113}, C_{114}, C_{123}, C_{124}, C_{144}, C_{133}$ $C_{134}, C_{155}, C_{222}, C_{333}$
Orthorhombic	$C_{111}, C_{112}, C_{113}, C_{122}, C_{123}, C_{133}, C_{222}, C_{223}$ $C_{223}, C_{333}, C_{144}, C_{155}, C_{166}, C_{244}, C_{255}$ $C_{266}, C_{344}, C_{355}, C_{366}, C_{456}$

3. Stresses. According to Murnaghan[4], the stress tensor is

$$\sigma_{ik}=\frac{\rho}{\rho_0}Y\left(\frac{\partial U}{\partial u_{ik}}\right)Y^*, \tag{6}$$

where ρ and ρ_0 are the densities in the deformed and undeformed states, respectively, $\rho=\rho_0(1+I_1)$, $Y=|\partial u_i/\partial x_k+\delta_{ik}|$, and Y^* is the transpose of the matrix Y.

When cubic terms in the strain are taken into account in the internal energy, the generalized Hooke's law (6) has, besides linear terms, also terms that depend quadratically on the strains, and these determine the elastic nonlinear effects in solids.

4. Equations of motion. The equation of motion has the usual form

$$\rho\frac{\partial^2 u_i}{\partial t^2}=\frac{\partial\sigma_{ik}}{\partial x_k}. \tag{7}$$

In the general case, for an isotropic solid, Eq. (7) takes the form[35]

$$\rho_0\frac{\partial^2 u_i}{\partial t^2}-\mu\frac{\partial^2 u_i}{\partial x_k\partial x_k}-\left(K+\frac{\mu}{3}\right)\frac{\partial^2 u_i}{\partial x_l\partial x_i}$$
$$=\left(\mu+\frac{A}{4}\right)\left(\frac{\partial^2 u_l}{\partial x_k\partial x_k}\frac{\partial u_l}{\partial x_i}+\frac{\partial^2 u_l}{\partial x_k\partial x_k}\frac{\partial u_i}{\partial x_l}+2\frac{\partial^2 u_l}{\partial x_k\partial x_k}\frac{\partial u_l}{\partial x_k}\right)$$
$$+\left(K+\frac{\mu}{3}+\frac{A}{4}+B\right)\left(\frac{\partial^2 u_l}{\partial x_i\partial x_k}\frac{\partial u_l}{\partial x_k}+\frac{\partial^2 u_k}{\partial x_l\partial x_k}\frac{\partial u_i}{\partial x_l}\right)$$
$$+\left(K-\frac{2\mu}{3}+B\right)\frac{\partial^2 u_i}{\partial x_k\partial x_k}\frac{\partial u_l}{\partial x_l}+\left(\frac{A}{4}+B\right)$$
$$\times\left(\frac{\partial^2 u_k}{\partial x_l\partial x_k}\frac{\partial u_l}{\partial x_i}+\frac{\partial^2 u_l}{\partial x_i\partial x_k}\frac{\partial u_k}{\partial x_l}\right)+(B+2C)\frac{\partial^2 u_k}{\partial x_i\partial x_k}\frac{\partial u_l}{\partial x_l}. \tag{8}$$

The nonlinear terms in the right-hand side of (8) do not vanish when all the three third-order moduli vanish, since the connection between the strain-tensor components and the displacements (1) is nonlinear. This geometrical nonlinearity is due to features of finite strains in solids.

In crystals, Eq. (7) is too cumbersome to be given here (see[36]).

III. THEORY OF NONLINEAR WAVES IN SOLIDS

The nonlinear equation (8) is usually solved by successive approximations: it is assumed that the ratio of the displacement amplitude u_0 to the sound wavelength λ (the acoustic Mach number) is sufficiently small. Then the terms $(1/c_0^2\cdot\partial^2u/\partial t^2)$ and $\partial^2u/\partial x_i\partial x_k$, in (8) where c_0 is the phase velocity of the wave, are of the order of u_0/λ^2. Since the ratio of the third- and second-order elastic moduli does not exceed several times ten, the nonlinear terms of the type $(\partial^2u/\partial x_i\partial x_p)(\partial u/\partial x_p)$ are of the order u_0^2/λ^3, i.e., of second order of smallness compared with the linear terms.

We represent the displacement in the form of a sum

$$u=u'+u''+u'''+\ldots, \tag{9}$$

the prime denoting the order of smallness, for example, $u''\sim u'u_0/\lambda$. Substituting (9) in (8), we obtain the first-approximation equation

$$\rho_0 \frac{\partial^2 u_i'}{\partial t^2} - \mu \frac{\partial^2 u_i'}{\partial x_k \partial x_k} - \left(K + \frac{\mu}{3}\right) \frac{\partial^2 u_i'}{\partial x_l \partial x_i} = 0. \qquad (10)$$

The second-approximation equation has the same form as (8), but the quantities in the left-hand side are of second order of smallness, and those in the right-hand side of first order of smallness. Thus, the problem reduces to a solution of system of linear equations with appropriate boundary conditions. In the first approximation this is the usual wave equation (10), and in the second approximation it is the inhomogeneous wave equation, since the known solution of Eq. (10) is substituted in the right-hand side of (8).

1. Nonlinear interaction of waves propagating in one direction. We shall henceforth consider a plane traveling wave propagating in the direction of the Ox axis. The second-approximation equations (8) then take the form[35]

$$\frac{\partial^2 u_x''}{\partial t^2} - c_l^2 \frac{\partial^2 u_x''}{\partial x^2} = \beta_l \frac{\partial^2 u_x'}{\partial x^2} \frac{\partial u_x'}{\partial x} + \beta_\tau \left(\frac{\partial^2 u_y'}{\partial x^2} \frac{\partial u_y'}{\partial x} + \frac{\partial^2 u_z'}{\partial x^2} \frac{\partial u_z'}{\partial x} \right), \qquad (11)$$

$$\frac{\partial^2 u_y''}{\partial t^2} - c_\tau^2 \frac{\partial^2 u_y''}{\partial x^2} = \beta_\tau \left(\frac{\partial^2 u_y'}{\partial x^2} \frac{\partial u_x'}{\partial x} + \frac{\partial^2 u_x'}{\partial x^2} \frac{\partial u_y'}{\partial x} \right), \qquad (12)$$

$$\frac{\partial^2 u_z''}{\partial t^2} - c_\tau^2 \frac{\partial^2 u_z''}{\partial x^2} = \beta_\tau \left(\frac{\partial^2 u_z'}{\partial x^2} \frac{\partial u_x'}{\partial x} + \frac{\partial^2 u_x'}{\partial x^2} \frac{\partial u_z'}{\partial x} \right), \qquad (13)$$

where

$$c_l^2 = \left(K + \frac{4}{3}\mu\right) / \rho_0, \quad c_\tau^2 = \mu/\rho_0, \quad \beta_l = 3c_l^2 + \frac{1}{\rho_0}(2A + 6B + 2C), \quad \beta_\tau = c_\tau^2 + \frac{1}{\rho_0}\left(\frac{A}{2} + B\right).$$

For a cubic crystal, a "pure" longitudinal wave can propagate in the directions [100], [110], and [111]. If the axis is directed along any of these directions, then the second-approximation equation can be written in the form (11) with $u_y = u_z = 0$ and with the values of c_l^2 and β_l listed in Table IV[37]. For directions differing from those indicated, the form of the equation does not change, but the coefficients in this case have a more complicated form[38].

It follows from (11) that propagation of a plane longitudinal wave ($u_y = u_z = 0$) excited by a source at $x = 0$, $u_x'(0, t) = u_0(1 - \cos \omega t)$ causes generation of a second longitudinal harmonic

$$u_x'' = -\frac{\beta_l}{c_l^2} \frac{x k_l^2 u_0^2}{8} [1 - \cos 2(\omega t - k_l x)], \qquad (14)$$

where $k_l = \omega/c_l$ is the wave number of the longitudinal wave. The solution (14) was obtained with the boundary condition $u_x''(0, t) = 0$. The linear growth of the second harmonic with increasing distance is due to the fact that no account was taken of the sound absorption. If sound absorption is taken into account, then (14) takes the form[39]

Table IV. Coefficients of second-approximation equation for cubic crystals

Wave propagation direction	c_l^2	$\beta_l - 3c_l^2$
[100]	c_{11}/ρ_0	C_{111}/ρ_0
[110]	$(c_{11}+c_{12}+2c_{44})/2\rho_0$	$(C_{111}+3C_{112}+12C_{166})/4\rho_0$
[111]	$(c_{11}+2c_{12}+4c_{44})2\rho_0$	$\frac{(C_{111}+6C_{112}+12C_{144}+24C_{166}+2C_{123}+16C_{456})}{9\rho_0}$

$$u_x'' = \frac{\beta_l k_l^2 u_0^3}{16 \alpha_l c_l^2} (e^{-2\alpha_l x} - e^{-4\alpha_l x}) [1 - \cos 2(\omega t - k_l x)], \qquad (15)$$

where $\alpha_l = (4\eta/3 + \eta')\omega^2/2\rho_0 c_l^3$ is the attenuation coefficient of the longitudinal wave, and η and η' are respectively the shear and bulk viscosity coefficients. At small $\alpha_l x$, Eq. (15) goes over into (14), i.e., the second harmonic increases linearly with the distance; then the growth rate is slowed down by dissipative losses. At a distance

$$x_s = \ln 2/2\alpha_l \qquad (16)$$

the second harmonic reaches a maximum and then decreases. It is possible to consider analogously the occurrence of combination (summary or difference) frequencies following simultaneous excitation of two longitudinal waves of different frequencies, propagating in the same direction in the solid. We note that, just as in liquids, when a longitudinal wave of sufficiently high intensity is excited in the solid, there should arise, besides the second longitudinal harmonic, also longitudinal higher harmonics—third, fourth, etc. The wave, just as in the liquid, gradually assumes a sawtooth form. The generation of these harmonics, as well as the formation of the sawtooth wave, cannot be described, strictly speaking, within the framework of the five-constant theory of elasticity; it is necessary for this purpose to take into account elastic moduli of higher order.

When the source excites only a transverse wave, polarized for example along the Oz axis ($u_x = u_y = 0$), the second-approximation equation (13) is the homogeneous wave equation. At zero boundary conditions it has only a zero solution, i.e., a transverse wave in an anisotropic body does not generate a transverse second harmonic. This result is quite obvious, since harmonic generation becomes impossible if the stress changes in absolute magnitude when the displacement sign is reversed. Since the absolute magnitude of the shear stress does not change when the shear direction is reversed, no second harmonic is generated. This holds true for an ideal isotropic solid. It can be shown that no transverse second harmonic is generated in cubic crystals (class m3m) in which a wave propagates only the directions [100], [010], [001] and in the directions of the face diagonals [110], [101], and [011]. In real solids, owing to residual internal stresses and dislocations, the generation of a second transverse harmonic can be observed experimentally (see Chapter IV)[40].

It follows from the form of (11) that a shear wave gives rise to longitudinal oscillations of double the frequency. This, however, is a typical example of the non-synchronous nonlinear effect*, since the propagation velocity of the induced process (the longitudinal wave) differs from the propagation velocity of the inducing transverse wave. Indeed, at $u_x' = u_y' = 0$ and $u_z'(0, t) = w_0(1 - \cos \omega t)$, the solution of the first-approximation equation has the usual traveling-wave

*Nonlinear wave interactions can be accompanied by synchronous processes in which the resultant wave is continuously amplified in the interaction region. Synchronous generation in three-wave interaction is determined by the conditions (20); if they are not satisfied, then the process is not synchronous (there is no continuous amplification of the wave at the combination frequency).

form. The solution of the second-approximation equation (11) is[35]

$$u_x'' = \frac{\beta_\tau k_\tau w_0^2}{4c_\tau^2(a^2-1)} \sin[(k_\tau - k_l)x] \cos[2\omega t - (k_\tau + k_l)x], \quad (17)$$

where $a = c_l/c_T$. The absence of synchronism causes the resultant harmonic to be "amplitude modulated" in space, and the period of the "modulation" is

$$\Delta x = \lambda_l/2(a-1), \quad (18)$$

where λ_l is the length of the longitudinal sound wave at the frequency ω. Since for most solids $a \sim 2$, the period (18) is $\sim\lambda_l/2 \sim \lambda_T$, i.e., the period of the "modulation" is of the order of the transverse wavelength. When the damping is taken into account, the longitudinal oscillations of double the frequency are given by[39]

$$u_x'' = \frac{\beta_\tau k_\tau w_0^2}{8c_\tau^2(a^2-1)} [e^{-4\alpha_l x} \sin 2(k_l x - \omega t) - e^{-2\alpha_\tau x} \sin 2(k_\tau x - \omega t)]. \quad (19)$$

The spatial oscillations then become smoothed out by the exponential factor. We shall henceforth call these "modulated" harmonics complicated harmonics.

We note that "modulated" harmonics are generated in the nonsynchronous nonlinear effects also in media having dispersion, for example, in nonlinear optics[41], and in the propagation of capillary waves on the surface of a liquid[42,43]. It is possible to let c_T in (17) formally tend to c_l. Then, as the difference between these velocities decreases, the period of the oscillations of the second-harmonic amplitude increases more and more, and finally, on going over to synchronous excitation $c_T = c_l$, Eq. (17) goes over into (14) for $\beta_T = \beta_l$ and $w_0 = u_0$.

If longitudinal and transverse waves propagating in the same direction are simultaneously excited, the interaction of the primary waves generates in second approximation, besides the longitudinal second harmonic (14) and the complicated longitudinal wave (17) due to the transverse wave, also a complicated transverse harmonic[39] whose spatial "modulation" period is $\sim 2\Delta x$, where Δx is given by (18).

Nonsynchronous nonlinear effects in isotropic solids, owing to the large difference between the velocities c_T and c_l, have, as seen from (18), a very small period of spatial oscillations. The "accumulation" of the generated harmonic during the propagation of the primary wave, which is characteristic of synchronous effects, is therefore missing. The amplitude of the complicated wave is quite small. An experimental observation of these waves is a very complicated task; these effects have not yet been observed in traveling waves.

2. Nonlinear interaction of intersecting waves (Raman scattering of sound by sound). We have considered above the interaction of plane traveling waves whose propagation direction was the same. This, generally speaking, is a particular case of the interaction. Two propagation velocities and three waves (one longitudinal and two transverse with mutually perpendicular polarization directions), a superposition of which can be used to represent any elastic wave in an isotropic solid, uncover great possibilities for synchronous nonlinear interaction of elastic waves when they intersect at different angles. As follows from the theory[5,44], the conditions for synchronous interaction

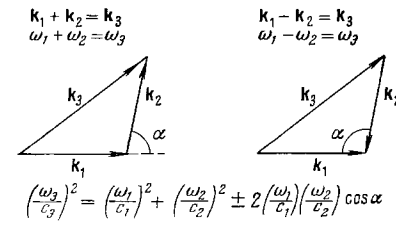

FIG. 1. Three-phonon interaction: the law of conservation of the energy and quasimomentum of phonons.

of excitation of a wave of frequency ω_3 with wave vector $\mathbf{k}_3$ under the influence of two plane waves ($\omega_1, \mathbf{k}_1$; $\omega_2, \mathbf{k}_2$) are as follows (Fig. 1)

$$\begin{aligned} \omega_1 \pm \omega_2 &\rightleftarrows \omega_3, \\ \mathbf{k}_1 + \mathbf{k}_2 &\rightleftarrows \mathbf{k}_3. \end{aligned} \quad (20)$$

When these conditions are satisfied, the transfer of energy from the interacting waves to the wave of combination frequency occurs in such a way that the amplitude of the generated wave increases continuously in the interaction region. The theory of[44] does not take absorption into account; it is qualitatively clear, however, that the absorption of the waves should impose an upper limit on the amplitude of the generated waves. The general problem of nonlinear interaction of two waves has never been considered before, in so far as we know. The result of the interaction (20) is a traveling wave.

The first of these conditions determines the frequency of the combination wave, and the second the direction of its propagation. Conditions (20) are obtained also in a quantum-mechanical analysis of three-phonon processes, where they are interpreted respectively as the laws of conservation of the phonon energy and quasimomentum*. The interaction corresponding to conditions (20) could be called, by analogy with Raman scattering of light, Raman scattering of sound by sound, for here, too, the direction and frequency of the scattered sound, generally speaking, differ from the directions and frequencies of the interacting sound waves.

We note that in media where there is only speed of sound (gases and liquids), the condition (20) admits of the interaction of only waves propagating in one direction; Eq. (20), naturally, is valid only for plane monochromatic waves. In the case of non-plane waves (e.g., sound beams) and non-monochromatic waves (e.g., when working with pulses), a certain deviation from conditions (20) is permissible; the degree of this deviation depends on the degree of non-monochromaticity and non-planarity of the wave. Under the experimental conditions one can produce waves that are sufficiently close to plane and monochromatic; then the deviation from (20) is determined by the experimental conditions.

The conditions (20) are necessary but far from sufficient for a nonlinear interaction of two waves accompanied by formation of a traveling wave of combination frequency. These conditions, for example, admit of generation of a second transverse harmonic,

*In the analysis of thermal phonons of high energy (high frequency), the momentum, as is well known, is conserved accurate to the reciprocal-lattice vector. For low-energy phonons, in which we are interested, there is no need to take these Unklapp processes into account.

which, as shown above, should not occur in an isotropic body.

The solution of the equations of the nonlinear theory of elasticity for two intersecting waves was found in[44,45]. Three-phonon interactions were considered quantum-mechanically in[46-49]. As shown in[45], when account is taken of the three polarizations of the interacting and scattered waves, and also of the formation of both summary and difference frequencies, one can conceive of a total of 54 types of interactions in an isotropic solid (Table V). Some of these interactions, however, are forbidden. The reasons for forbiddenness are: A) failure to satisfy the synchronism conditions (20) (or, equivalently, failure to satisfy the conservation laws for the energy and quasimomentum of the interacting phonons); B) failure to satisfy the polarization conditions. Some of the interactions (C) are possible only when the waves propagate in one direction. Finally, some interactions (D) are possible for intersecting waves. In Table V the transverse waves polarized in the interaction plane are designated T, while those polarized perpendicular to the interaction plane are designated T'. We note that the table lists the results of the analysis of the interactions only from the point of view of satisfaction of (20) and of the polarization conditions, while the interaction efficiency (or, using the quantum-mechanical terminology, the interaction probability) was not taken into account. It is seen from Table V that out of the 54 types of interaction, 36 are completely forbidden, 10 are possible only when the waves propagate in the same direction, and finally 8 are possible for intersecting waves. The interaction of waves propagating in the same direction was considered in part in the preceding section. We emphasize here that in a lossless medium the interaction of waves propagating in the same direction is in principle not subject to any limitation on the frequencies of the interacting waves: waves of very low frequency can interact with waves of very high frequency, producing combination frequencies. When absorption is taken into account, obviously, it is meaningful to speak of interactions only in the case when the mean "free" path of one of the waves, with high frequency, $\sim \alpha_1^{-1}$, where α_1 is its absorption coefficient, is larger than the length of the other (low-frequency) wave λ_2, i.e., $\alpha_1\lambda_2 \ll 1$. In the opposite case the first wave has time to attenuate before the parameters of the medium can be modified significantly in any way under the influence of the second wave.

Unlike the interaction of waves propagating in the same direction, Raman scattering, generally speaking, is limited by a large number of conditions, and when these conditions are satisfied, it is possible for a limited region of interacting-wave frequencies.

As already mentioned in the Introduction, we confine ourselves in this review to only phonon-phonon interactions and we have considered above only the elastic nonlinearity due to the lattice anharmonicity. In hypersonic investigations, however (see Ch. IV), one encounters a problem in which a definite role can be played (e.g., in the investigation of the generation of harmonics in piezoelectric crystals) by harmonic generation due to causes other than the anharmonicity of the lattice. Such causes include electrostriction and

Table V. Forbidden and allowed three-phonon scattering processes for an isotropic solid

No.	Interaction waves		Scattered waves					
			$\omega_1+\omega_2$			$\omega_1-\omega_2$		
			L	T	T'	L	T	T'
1	$L(\omega_1)$	$L(\omega_2)$	C	A	B	C	D	B
2	$L(\omega_1)$	$T(\omega_2)$	D	A	B	D	D	B
3	$T(\omega_1)$	$L(\omega_2)$	D	A	B	A	A	B
4	$T(\omega_1)$	$T(\omega_2)$	D	C	B	A	C	B
5	$T'(\omega_1)$	$T'(\omega_2)$	D	C	B	A	B	C
6	$L(\omega_1)$	$T'(\omega_2)$	B	B	A	B	B	D
7	$T'(\omega_1)$	$L(\omega_2)$	B	B	A	B	B	A
8	$T'(\omega_1)$	$T(\omega_2)$	B	B	C	B	B	C
9	$T(\omega_1)$	$T'(\omega_2)$	B	B	C	B	B	C

nonlinear piezoelectric effects, which can play a definite role, for example, in the excitation of hypersound on the surface of a piezoelectric crystal partly placed in a resonator. In addition, the alternating component of the radiation pressure of an electromagnetic wave of frequency equal to the second harmonic can turn out to be significant theoretically. These questions are considered in[50,51], where expressions are given for the second-harmonic amplitude. In these expressions, besides the elastic nonlinearity, account is taken also of the electrostriction, the pressure of the electromagnetic radiation, and the nonlinearity of the piezoelectric effect. We shall not stop to discuss this here, since we were unable to observe in our measurements, at frequencies on the order of 10^9 Hz, the influence of these factors on the second-harmonic amplitude (see Ch. VI), at least for longitudinal waves, even in such a strong piezoelectric and ferroelectric as lithium niobate (at room temperatures). It is possible, incidentally, that in other cases these factors are of definite significance.

3. Stimulated standing waves of finite amplitude in solids. Other conditions being equal, nonlinear acoustic effects in solids are as a rule weaker by 1—2 orders of magnitude than in liquids. To separate the harmonics, it is necessary to use here more sensitive apparatus. This is discussed in detail in Ch. IV, where experimental methods for studying nonlinear wave phenomena in solids are discussed. We mention here that nonlinear effects in resonant acoustic systems, especially for stimulated oscillations near resonant frequencies and at high resonator Q values, become much more strongly manifest than in a wave traveling in an unbounded medium[52-55]. This uncovers additional possibilities for investigating nonlinear properties of solids. It was shown in[54] that at Reynolds numbers $\mathrm{Re} = ku_0 \cdot kL \cdot Q$ larger than unity (u_0 is the amplitude of the vibrational displacement exciting the resonator, L its length, and Q the quality factor of the resonator), the nonlinear effects are manifest in harmonic generation, and in the possibility of resonant excitation at frequencies different from the linear resonant frequencies. When $\mathrm{Re} > 1$ all these effects are quite clearly pronounced. The use of resonant oscillations is a very sensitive method of separating nonlinear effects.

Longitudinal and transverse waves of finite amplitude in a solid layer, and also nonlinear detection of

an amplitude-modulated sound wave by means of a solid rod excited by a longitudinal or a transverse wave, were considered in[55] with accuracy to quantities of second order of smallness. In particular, if longitudinal or transverse standing waves of high frequency ω modulated by low frequency Ω, which is the natural frequency of the rod, are excited in a solid rod clamped at midpoint, then three waves propagate in the rod, the carrier ω and the two sideband frequencies $\omega \pm \Omega$. These waves interact in nonlinear fashion with one another and the nonlinear elasticity of the rod causes acoustic detection (separation of the low frequency Ω). The amplitude of the longitudinal oscillations of a rod of length L at a low frequency Ω, $u''_{\Omega}|_{x=L}$, turns out in this case to equal

$$u''_{\Omega}|_{x=L} = \frac{\beta_i u_0^2 m\omega^2 \frac{c_0}{c}\left(\cos\frac{\Omega L}{c}\cos\frac{\Omega L}{c_0}\right)}{8\Omega\left(1-\frac{c_0^2}{c^2}\right)} \frac{t}{\sin\frac{\Omega L}{c_0}}\cos\Omega t \times\left\{\frac{\cos k_1 L}{\operatorname{ch} 2\alpha L+\cos 2k_1 L}\left[\frac{\cos k_2 L}{\operatorname{ch} 2\alpha L+\cos 2k_2 L}-\frac{\cos k_3 L}{\operatorname{ch} 2\alpha L+\cos 2k_3 L}\right]\right\}. \quad (21)$$

Here $\beta_i = \beta_l$, $\alpha = \alpha_l$, and $c = c_l$ if a longitudinal high-frequency wave is excited in the rod, and $\beta_i = \beta_T$, $\alpha = \alpha_T$, and $c = c_T$ if a transverse wave is excited, where c_0 is the velocity of the longitudinal waves in the thin rod, m is the depth of modulation, $k_1 = \omega/c$, $k_2 = (\omega + \Omega)/c$, and $k_3 = (\omega - \Omega)/c$. In deriving this expression it was assumed that the damping of the sound of fundamental frequency is small over the length of the rod, $\alpha L \ll 1$.

In concluding this chapter, let us discuss some experimentally observable features that follow from the theoretical results given above on nonlinear effects in solids. First, is the observation of second longitudinal harmonics generated in a longitudinal wave. From (15) we find that at the stabilization distance the harmonic displacement amplitude reaches a maximum value

$$(u''_x)_{\max} = \frac{\beta_l k_l^2 u_0^2}{64\alpha_l c_l^2} = \frac{\varepsilon_l \rho c_l u_0^2}{16\eta} = \frac{\varepsilon_l}{32\pi}\operatorname{Re} u_0,$$

where $\epsilon_l = \beta_l/2c_l^2$ is a dimensionless nonlinear parameter, $\eta = 2\alpha_l \rho c_l^3/\omega^2$ is the effective viscosity, Re $= \rho\omega u_0\lambda/\eta$ is the acoustic Reynolds number, and λ is the wavelength.

We see from this relation that $(u''_x)_{\max}/u_0 \sim$ Re, i.e., this ratio depends on the vibrational velocity produced by the sound source and by the effective viscosity of the solid. As a characteristic example, we present the value of $(u''_x)_{\max}$ for a magnesium-aluminum alloy at ~ 4.5 MHz. For this alloy $\epsilon_l \approx 6$, $\alpha_l = 8 \times 10^{-3}$ cm^{-1}, and $c_l = 6.26 \times 10^5$ cm/sec. From (16), the stabilization distance is $\sim$44 cm. At this distance $(u''_x)_{\max} \approx 4.3 \times 10^4\, u_0^2$; if the voltage on the quartz radiator is on the order of several hundred volts, then $u_0 \approx 10^{-7}$ cm, i.e., $(u''_x)_{\max}/u_0 = 4.3 \times 10^{-3}$. At 4.5 MHz, the magnesium-aluminum alloy has very small damping. Measurements in solids with large damping is made difficult not only by the fact that the maximum amplitude of the harmonics is small, but also by the fact that the stabilization distance (16) is small in this case, when it is practically impossible to carry out measurements by the pulsed spectral method at distances smaller than or equal to the stabilization distance. On the other hand, work in a region more remote than the stabilization distance causes the amplitude of the harmonics to be much smaller than the maximum value. It is useful to bear this in mind when choosing the frequency band for the investigation of the harmonics.

Nonsynchronous generation of a harmonic of the type (17) leads, owing to the absence of accumulating effects, to very weak distortions even in solids with small damping. An estimate of $(u''_x)_{\max}$ for this case can be obtained by assuming that the distance over which the harmonic grows is $\sim \Delta x/2$, where Δx is the period of the spatial "modulation" (18), at the characteristic conditions considered above, and at $u_0 \approx 10^{-7}$ cm, we get $(u''_x)_{\max}/u_0 = 10^{-5}$, which is lower by two orders of magnitude than the corresponding value in synchronous generation of the second harmonic.

A few words concerning the observation of Raman scattering of sound by sound. In spite of the fact that this is a synchronous effect, the amplitude of the generated wave at the combination frequency is here as a rule smaller than the maximum amplitude of the synchronously generated second harmonic, owing to the fact that the interaction region of the waves is smaller here. It has already been noted above that there is at present no theory of Raman scattering with allowance for damping. However, it is possible that since the amplitude of the displacement of the combination wave is $\sim \omega^3$, it would be possible to obtain a large effect at high frequencies. It must be said that although the ratio of the amplitude of the combination wave to the amplitude of the interacting waves is smaller here by at least one order of magnitude than the analogous quantity in second-harmonic generation, the separation of a useful signal is a much simpler matter, since there are more possibilities for verifying that the interaction occurs in the medium (the reception direction, the generally non-integer ratio of the frequencies, etc. see below).

IV. EXPERIMENTAL METHODS AND CERTAIN RESULTS OF AN INVESTIGATION OF NONLINEAR WAVE PHENOMENA IN SOLIDS

At the present time there are already several dozen experimental papers devoted to nonlinear phenomena occurring when elastic waves propagate in solids. In this chapter we shall stop briefly to discuss investigation of harmonic generation and generation of combination frequencies (both at ultrasonic and hypersonic frequencies), the generation of transverse harmonics due to crystal defects, combination scattering of sound by sound, generation of harmonics in Rayleigh waves, and nonlinear resonances in acoustic resonators. Finally, we shall describe recently developed optical-acoustic methods for investigating nonlinear phenomena in the propagation of elastic waves.

1. Study of the generation of harmonics of longitudinal waves by the pulsed spectral method. In the first studies of nonlinear acoustic effects in solids, a pulse spectral method was used[2,56]. A block diagram of the simplest setup for the observation of harmonic genera-

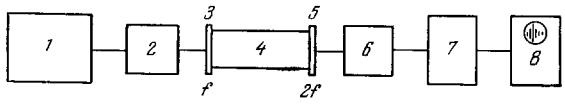

FIG. 2. Block diagram of pulsed-spectral method of measuring harmonics at ultrasound frequencies.

tion by such a method is shown in Fig. 2. The measurement procedure itself may seem at first glance to be very simple. However, owing to the relatively small nonlinearity of the solids, the harmonics produced when sinusoidal (at the radiator) elastic waves propagate are small, and certain difficulties are involved in proving that the harmonic generation occurs precisely in the solid and is not connected with the nonlinearity of the apparatus.

Figure 2 illustrates application of a radio pulse to a piezoelectric plate 3 via a resonant circuit (rejection filter) 2, which suppresses the possible second harmonic of the sinusoidal-voltage generator 1. The amplitude of the pulse applied in[2] to an X-cut quartz plate was 1000 V, but it is possible (using an amplifier of higher sensitivity) to operate at voltages on the order of only several dozen volts. Ultrasonic pulses (with carrier frequency of several MHz) pass through a solid sample 4 and are then received by piezoelectric plate 5, the resonant frequency of which, 2f, is double the fundamental frequency. The received pulse passes then through a rejection filter 6, which suppresses the signal of the fundamental frequency f, and is fed to a resonant amplifier 7. This amplifier is tuned to the second-harmonic frequency 2f and its gain 1000. The second-harmonic pulses produced at the output of this amplifier by the elastic nonlinearity in the sample are then fed to the indicator 8. The character of the envelope of the series of pulses resulting from multiple reflection from the end of the sample depends on the impedances of these ends[29,37,50]. The simplest case is that of infinite impedance. Then the phase relations between the first, second, and higher harmonics remain unchanged by reflection, and the second harmonic (as well as the higher harmonics) increases with increasing path traversed by the pulse. As the path is increased, the dissipative losses assume an increasing role. In this case, if the length of the sample is shorter than the stabilization distance given by (18), one observes a series of pulses, which first increase (up to the stabilization distance) and then decrease. The situation is somewhat more complicated if the impedance of the end face opposite to the ultrasound source is equal to zero (the boundary is absolutely free). On reflection from a boundary with zero impedance, the phase relations between the first and second harmonics change for longitudinal waves in such a way that after reflection the second harmonic begins to decrease. Were there no attenuation, then a purely sinusoidal wave would return to the radiator (with a zero second-harmonic amplitude). If the reception of the second harmonic is at a boundary with zero impedance, then the amplitude of the first-harmonic pulses decreases exponentially (the amplitude of the pulses would remain constant without attenuation). In the case of finite impedance of the reflecting end, the envelope of the pulses is intermediate between an exponentially-decreasing one (zero impedance) and a curve with a maximum (infinite impedance). Under the experimental conditions it is easier to realize the case of a free boundary, especially when working with hypersonic frequencies (see below).

We note that the phase of a transverse wave reflected from a free boundary remains unchanged, and therefore the second-harmonic amplitude for transverse waves should continue to increase up to the stabilization distance also after reflection from ends having zero impedance. In the reception of the second harmonic as shown in Fig. 2, the impedance of the receiving end of the sample depends significantly on the features of the acoustic contact between the plate 5 and the sample; the end of the sample is here in contact with a liquid film (if longitudinal waves are received) or a solid splice (when transverse waves are received). Located behind the film is a resonant plate for the second harmonic (quarter-wave plate for the first harmonic). Under certain conditions, the latter makes it possible to obtain a sufficiently high impedance, at which a growing series of second longitudinal harmonic pulses can be observed.

Figure 3 shows such a series of second-harmonic pulses (longitudinal waves) in a sample of magnesium-aluminum alloy[2]*. As the wave traverses the distance from the radiator, the second-harmonic pulses increase, reach a maximum (stabilization distance determined by (16)), and then decrease as a result of the predominant influence of the dissipative processes. We note that in this study the dependence of the second-harmonic amplitude on the distance traversed by the wave was determined also for samples with different lengths (leaving the experimental conditions unchanged). Figure 4 shows this dependence in rods of magnesium-aluminum alloy of different lengths (fundamental frequency 5 MHz).

In the cited paper[2], the measured value of the second-harmonic amplitude and expression (14) were used to determine the ratio of the combination of three third-order elastic moduli ϵ_l to the second-order moduli for a number of single crystals (Al, NaCl, KCl, LiF), which turned out to be in good agreement with Bridgman's data obtained from measurements of the hydrostatic compressibility.

At hypersonic frequencies, a number of indirect symptoms of nonlinear distortion and interaction of hypersonic waves of frequency 9×10^9 Hz at helium temperatures were observed in[57], for example, an increase of the absorption with increasing hypersound intensity.

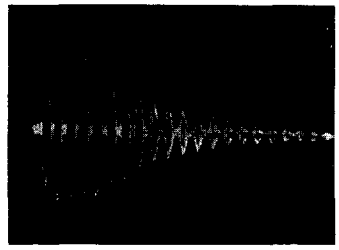

FIG. 3. Series of second-harmonic pulses (10 MHz) in magnesium-aluminum alloy. Voltage of 5 MHz radiator is 1000 V (maximum). Rod length 7.5 cm.

*Calculated sound intensity ~1 W/cm², sound-pressure amplitude ~6 atm, vibration-displacement amplitude ~7×10^{-8} cm.

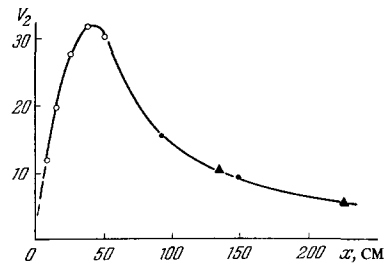

FIG. 4. Dependence of the amplitude (voltage V_2 on the receiving plate in mV) of the second harmonic (10 MHz) on the distance from the radiator in magnesium-aluminum alloy at a radiator voltage 1000 V: ○–determined from amplitude of first pulse on rods of different lengths, ●–second and third pulses on a rod 30 cm long, ▲–second and third pulses on a rod 45 cm long.

The first experiments with the pulsed spectral procedure, analogous to the procedure used in[1,2] at ultrasonic frequencies, were performed for hypersound in[58,59]. In these investigations, at helium temperatures, second-harmonic generation was observed in X-cut quartz. The excitation of the quartz (as well as the reception of hypersound) was by placing the crystal in a microwave resonator at the antinode of the high-frequency electric field, i.e., from the surface of the crystal. This method, developed by K. N. Baranskii[60] and further extended in[61] by different modifications, is now widely used. A second harmonic was observed, however in[58,59] and was attributed by the author to nonlinear phenomena occurring on the crystal surface itself when the crystal is surface-excited. Further research, including some by Carr himself[50], does not confirm this conclusion.

Let us stop to discuss briefly the experimental procedure used by us[62]; a similar procedure was used in other investigations[50,63,64]. Figure 5 shows a block diagram of a setup for observing at 400 MHz harmonic generation in a single-domain crystal of lithium niobate in which hypersound propagates along the z axis. Here PG is a pulse generator, HFG a high-frequency generator, DL a delay line. The receiving channel consists of a heterodyne H, a mixer M, an intermediate-frequency amplifier IFA, and a detector D. The bandwidth of the receiving channel is 4 MHz, the maximum sensitivity is 10^{-12} W, R_1 and R_2 are coaxial resonators, and Cr is a single-domain $LiNbO_3$ sample. The excitation and reception of the waves were effected from the surface, in resonators R_1 and R_2 tuned respectively to the signal frequency and to double this frequency. A rejection filter (attenuation 48 dB) is connected in the channel between HFG and R_1 and is tuned to the frequency of the second harmonic, so as to exclude the excitation of the crystal by the double frequency due to the nonlinear distortion factor of the generator. A rejection filter tuned to the fundamental frequency (attenuation 25 dB) is connected between R_2 and M to prevent appearance of a false second harmonic in the receiving channel. The $LiNbO_3$ crystal had a diameter 1.3 cm and a length 3.36 cm. The ends of the crystal were optically plane-parallel and polished. The radio pulse duration was 3 μsec, and the peak power on the order of several watts.

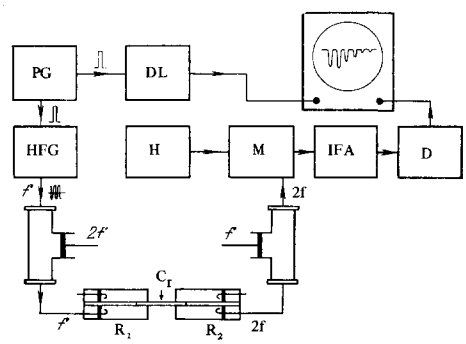

FIG. 5. Block diagram of pulsed-spectral method of measuring harmonics at microwave frequencies.

An oscillogram of a series of second-harmonic pulses is shown in Fig. 6. The first pulse is the probing pulse, and the second is the start of the series of longitudinal ultrasonic pulses at double the frequency; the third, sixth, and ninth pulses constitute a series of transverse double-frequency pulses, since both types of waves are simultaneously excited in the crystal. A number of control measurements have shown that the observed second harmonic is not due to different apparatus nonlinearities. The loss due to the double electromechanical conversion amounted to 50 dB at the fundamental frequency and about 65 dB at the double frequency. An estimate of the longitudinal second-harmonic radio-signal power at the receiver output gave values 10^{-9}–10^{-10} W for different conditions. The first-harmonic power was of the order of 10^{-6} W, meaning that the second-harmonic amplitude was (0.35–0.12)% of the first-harmonic amplitude. The intensity of the sound and other parameters of the sound field can be approximately calculated from the electromagnetic power and the losses to a single electromechanical conversion. Indeed, if the electromagnetic power is P_{em} and the conversion loss is γ, then $P_{ac} = \gamma P_{em}$. For a plane wave, the intensity, as is well known, is $Y = 2\pi^2\rho c^3(u_0/\lambda)^2$, where ρ is the density, c the speed of sound, $\xi = u_0/\lambda$ the amplitude of deformation in the acoustic field. From these relations we get $\xi^2 = P_{ac}/2\pi^2\rho c^3 S$ (S is the beam cross section area) and

$$\frac{\xi_2}{\xi_1^2} = \left[\frac{2\pi^2\rho c^3 S P_2}{P_1^2}\right]^{-1/2},$$

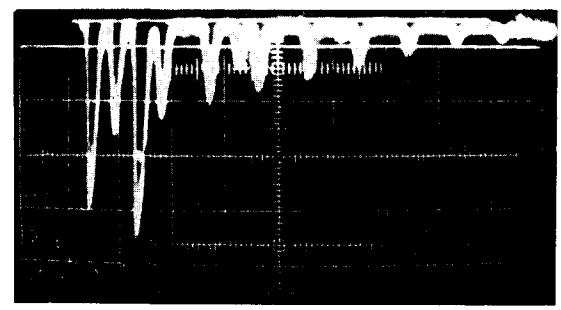

FIG. 6. Oscillogram of longitudinal and transverse second harmonic in $LiNbO_3$. Fundamental frequency f_1 = 400 MHz. Excitation from the surface, propagation along the z axis. Sample length 3.36 cm, diameter 1.3 cm. First pulse–induction, second–longitudinal wave, f_2–800 MHz, third–transverse wave, f_2 = 800 MHz, fourth and fifth–longitudinal and sixth–transverse.

where the indices 1 and 2 correspond to the first and second harmonics. This formula makes it possible to estimate the acoustic deformations and displacements from the measured electromagnetic power of first and second harmonics. In our case, at P_{em} on the order of several watts, the amplitudes of vibration displacements were of the order of 10^{-10} cm at the fundamental frequency and of the order of 10^{-13} at the second harmonic. The absolute parameters of the acoustic field were measured by applying to the receiving channel first the received signal and then an amplitude-calibrated signal from a separate generator. The formula given above makes it possible to determine ξ_2/ξ_1^2 from the first received pulse. The deformation amplitude for the second harmonic propagating along the z axis of the sample, at distances much smaller than the stabilization distances, is according to (14)

$$\xi_2 = \frac{1}{8}\Gamma_l \xi_0^2 x k_l^2 \lambda,$$

where $\Gamma_l = 3 + (C_{333}^D/c_{33}^D = -\beta_l/c_l^2$ is the effective nonlinear parameter (here c_{33}^D is the elastic modulus of second order, and C_{333}^D is the elastic modulus of third order at constant induction D). Using this relation, we can determine the effective value of the nonlinear parameter for $LiNbO_3$ along the z axis, namely, $\Gamma_l = 1.4 \pm 0.9$.

We note that in other investigations of harmonic generation at hypersonic frequencies there were no indications of excitation of a transverse second harmonic. A decreasing series of the second transverse harmonic is clearly seen on the oscillogram of Fig. 6. Generation of the transverse second harmonic under the influence of a transverse wave in an anisotropic solid or in a cubic crystal (for propagation in the directions [100], [010], [001], and [111]) is possible, as already indicated in Ch. III, only in the presence of imperfections in the crystal (dislocations, internal stresses, etc.). Under experimental conditions of this work, the transverse harmonic could result also from anisotropy.

When the electromagnetic pulse power was increased to 10 W, it was possible to observe also a third longitudinal harmonic at a frequency 1200 MHz.

In accordance with[50], the measured value of Γ for piezoelectrics and ferroelectrics may include, generally speaking, both the lattice nonlinearity and the nonlinearity that can result from surface excitation of hypersound. Therefore the separation of the lattice second harmonic entails certain difficulties in the case of surface excitation of piezoelectrics. Since, as already noted, the nonlinear effects are small, it is necessary to cope with a large number of other factors producing second harmonics on the surface of the crystal, not connected with the anharmonicity of the lattice.

We shall call this the surface harmonic. One of the causes of the occurrence of a surface harmnnic is the pressure of the electromagnetic radiation (since it is proportional to the square of the field intensity, we have here besides the fundamental component also a pressure component that varies at double the frequency). This second harmonic due to the pressure of the electromagnetic radiation could be observed experimentally by placing in a resonator one end of a non-piezoelectric dielectric (corundum), on the other end of which there was sputtered a film of cadmium sulfide used as a second-harmonic receiver[65]. Another cause of the generation of a surface second harmonic may be the electrostriction effect. This second cause must be particularly taken into account when hypersound is excited in ferroelectrics, particularly lithium niobate or tantalate. Finally, a third cause of excitation of a second harmonic on a surface of a piezoelectric crystal plate in a resonator may be the nonlinearity of the piezoelectric effect. Separation of the second harmonic due to the anharmonicity of the lattice is quite complicated also because of other already mentioned reasons.

Returning to[62], it should be pointed out that the correction for the radiation pressure of the electromagnetic waves, as shown by an estimate on the basis of[50], is smaller by three orders of magnitude for ξ_2/ξ_0 that its mean experimental value. Thus, the radiation pressure makes no essential contribution to Γ_l in the described experiments, even though it can lead in principle to the appearance of an acoustic second harmonic and was observed experimentally in corundum[65]. As to the electrostriction effect and the nonlinearity of the piezoelectric properties one can expect the surface second harmonic to make a definite contribution to the total second-harmonic amplitude, since lithium niobate is ferroelectric.

The value of the surface second harmonic can be determined for a piezoelectric sample by studying the behavior of the summary or difference frequencies appearing when two longitudinal or transverse waves propagating in the same direction interact. As proposed in[66], one can proceed for this purpose as follows: After applying a pulse of frequency f_1 to a converter at the instant of time t_0, a delay is introduced, amounting to the time 2τ required for the elastic pulse to traverse the length of the sample and to return to the radiator after reflection. At the instant $t_0 + 2\tau$, an electromagnetic pulse of frequency f_2 is applied. From that instant on, both pulses of frequency f_1 emitted at the instant t_0 and of frequency f_2 emitted at the instant $t_0 + 2\tau$—propagate in the crystal together, and a nonlinear interaction occurs between the waves of frequencies f_1 and f_2. This eliminates the possible nonlinear interaction and production of harmonics by electromagnetic excitation of the surface of the piezoelectric sample, since the electromagnetic pulses of frequencies f_1 and f_2 no longer act simultaneously at the surface of the piezoelectric. Using such a procedure for propagation in lithium niobate along the z axis and the setup described above[62] (see Fig. 5), we observed, together with K. K. Ermilin, the formation of longitudinal and transverse waves at the difference frequency 805 MHz by interaction of two collinear hypersonic beams with frequencies $f_1 = 1205$ MHz and $f_2 = 400$ MHz.

We call attention to the fact that excitation of the crystal led to simultaneous generation of both longitudinal and transverse waves. It turned out here that in the case of surface excitation of longitudinal waves, within a measurement error of not more than 5—7%,

it was impossible for a difference-frequency wave to occur as a result of electrostriction or nonlinearity of the piezoeffect.

2. Generation of transverse harmonic. According to nonlinear theory of elasticity, as shown in Ch. III, no generation of the second harmonic in a transverse wave should be observed in isotropic bodies in the second approximation. This is caused by the fact that there are no quadratic terms for the shear deformation in the nonlinear Hooke's law, owing to the equivalence of the shear in the forward and backward directions. We note that the phonon energy and quasimomentum conservation laws (20), as already indicated, admit of the possibility of "merging" of two transverse phonons having equally directed quasimomenta, but owing to the form of the elastic energy the probability of such an interaction is zero. In crystals, for an arbitrary propagation direction, interactions of this kind are in general not forbidden. It can be shown, however, that, say for a crystal of cubic symmetry of class m3m, there are definite directions [100] and [110] (in which the propagation of the "pure" shear wave is possible), where no transverse second harmonic generation occurs. Its generation becomes possible if a longitudinal wave propagates in addition to the shear wave (see Ch. III). This, however, is a case of nonsynchronous generation, and for traveling plane waves there is no spatially-growing second transverse harmonic; its amplitude varies periodically in space with a period on the order of the longitudinal wavelength. Nonsynchronous generation in solids, where the difference between the velocities of the longitudinal and transverse waves is large, leads to very small nonlinear effects.

Experiments have shown[40] that in solids with relatively small damping (polycrystalline magnesium-aluminum alloy, aluminum, duraluminum) and also in pure single crystals of aluminum (99.95% Al), cadmium, and zinc, a second shear harmonic can be relatively easily separated if sound propagates in the [100] direction. The magnitude of this harmonic is smaller by one or two orders of magnitude than the magnitude of the longitudinal harmonic generated in the longitudinal wave. In single crystals of metals, the amplitude of the generated harmonic observed in[40] was strongly dependent on relatively weak external actions—the local action of force or a small local heating.

The influence of an external force on an aluminum single crystal is shown in Fig. 7. The influence of the external force is too small to be able to propose some change in the lattice nonlinearity. In addition, the dependence of the effect on the point of application of the force, the characteristic relaxation effects (the increase of the shear-harmonic amplitude upon flexure of single crystals of cadmium and zinc, followed by a gradual slow return of the harmonic to its previous value after the removal of the force), all are characteristics of the defect structure of the crystal. We note that the stresses applied to the sample, as seen from Fig. 8, were smaller than the light slippage stresses, which for Al amount to several kg/mm^2. Still smaller (not more than several kg/cm^2) were the alternating shear stresses in the ultrasonic wave.

Although a second shear harmonic was indeed

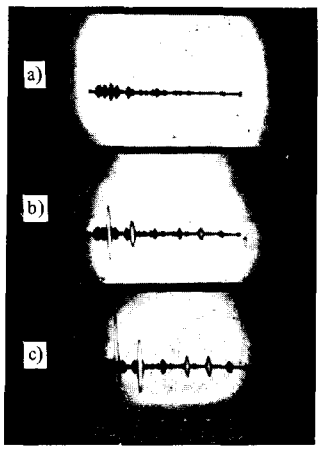

FIG. 7. Oscillograms of second shear harmonic in aluminum single crystal at different loads: a) without load, b) load 1 kg, c) load 5 kg. The direction of the force producing the load coincides with the direction of the wave polarization. The pulses of the second transverse harmonic are marked by the indices s_i (i is the number of the pulse); M is electrical interference. Pulses whose amplitude remains unchanged under load constitute the second harmonic of the longitudinal wave produced by external radiation of a longitudinal wave by means of a BT-cut quartz plate.

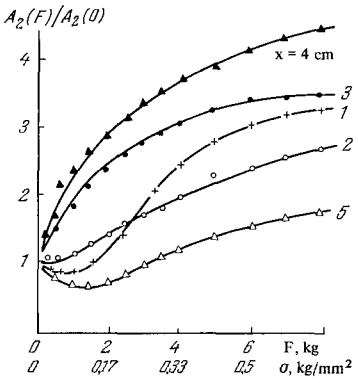

FIG. 8. Ratio of the amplitude of the second shear harmonic (under the influence of a force F), $A_2(F)$, to the harmonic in the presence of a force, $A_2(O)$, as a function of F for different distances from the sound source.

generated in polycrystalline metals, it was impossible to change its amplitude by means of weak external action; this indicates probably that the metal in the single-crystal grains is hardened to a sufficient degree and the stresses produced by the external forces are small compared with the internal stresses.

The microscopic role played by defects for phonon scattering is obvious: forbidden phonon-phonon interactions become possible near the defects. Macroscopically (for waves much longer than the dislocation dimension), the influence of the crystal effects can also be observed. The possible cause of this are the residual internal stresses produced by the dislocations. Their influence is qualitatively obvious; they cause Hooke's law for shear strains to contain, besides terms with odd powers of the strains, also terms with even powers, i.e., shear strains behave differently with respect to stresses of the same absolute magnitude, depending on the stress direction. The situation here becomes analogous to that of longitudinal waves, when different stresses have to be applied in order to obtain compression and rarefaction of equal absolute magnitude.

A shear second harmonic can arise only if the number of regions in the crystal, where the shear in a positive direction requires larger stresses than in the

opposite direction, when averaged over the crystal, is not equal to the number of regions of opposite sign*. In the propagation of an elastic wave, the latter "counts" all the regions; in the positive regions the phase of the harmonic is opposite to the phase in the negative regions. Qualitatively, this mechanism of generating the shear harmonic was confirmed also experimentally: 1) the action of an external force is most effective when the force direction coincides with the direction of the wave polarization; the action of the external force has practically no effect when its direction is perpendicular to the direction of the shear-wave polarization; 2) the integral character of the effect can be seen from the fact that the magnitude of the observed second harmonic depends not on the stress produced by the external force but on the force itself (the dimensions of the contact between the pressing rod and the crystal play no role, only the magnitude of the load matters).

It should be stated that the influence of an external static pressure depends naturally on the number and locations of the positive and negative regions for a given force direction and for a given shear-wave polarization. Therefore, application of an external static force at different points can both increase or decrease the generated second harmonic (see Fig. 8).

An analogous effect was subsequently observed in the propagation of longitudinal waves in single crystals and polycrystals of aluminum; the stretching (or compression) of the crystal in the propagation direction of the longitudinal ultrasound wave caused the second longitudinal harmonic to change[67]. Here, too, the static stresses are insufficient to attribute the observed phenomena to a change in the lattice nonlinearity. Like in the case of shear waves, they are due to the influence of the defect structure on the elastic nonlinearity of solids.

Notice should be taken of the double role played by the dislocations in the distortion of the finite-amplitude waves. At small external static stresses, prior to the detachment of the dislocations, the external stresses "bend" the dislocation loops more strongly and lead to an increase of the effective nonlinearity, and consequently to an increase of the amplitude of the generated wave. Further increase of the static stress leads to a detachment of the dislocations at the point where they are strongly pinned, and to an elongation of the dislocation loops as well as to the appearance of new dislocations. This increases not only the effective nonlinearity, but also the damping of the elastic wave. Other conditions (wave amplitude, frequency, etc.) being equal, this damping decreases the magnitude of the generated second harmonic.

Continuation of[40] in our laboratory has demonstrated that in aluminum crystals subjected to prior plastic deformation the second harmonic was more strongly dependent on small static stresses than prior to application of the plastic deformation. This result is natural, since prior plastic deformation increases the dislocation density. It should be stated that although plastic deformation greatly increases the number of dislocations, there is nevertheless no sharp increase in the number of the stressed microregions of the same sign, since the amplitude of the harmonic increases in this case by not more than 2–3 times.

In this respect, results obtained in our laboratory on lithium-fluoride crystals are also distinct. In alkali-halide crystals the dislocations are pinned more rigidly and these crystals, as a rule, are much less plastic. Therefore the action of an external static force (even much larger than in the case of aluminum crystals) in these crystals does not lead to a change in the transverse-harmonic amplitude. The influence of dislocations on the generation of a transverse harmonic can be determined here by using samples with different dislocation densities. One of the main difficulties in performing experiments of this type is the creation of identical radiation and reception conditions, so as to be able to compare the results.

More or less equal conditions were attained in these experiments by effecting the reception through a buffer made of fused quartz, and effecting the contact between the radiator and the samples and between the samples and the buffer with the aid of vacuum grease (this introduced an error of ~ 5–7% in the measurements). The magnitude of the second transverse harmonic was determined in an unhardened LiF single crystal with dislocation density 10^3–10^4, in a medium-hardened LiF sample with dislocation density 10^4–10^5, and in a strongly hardened LiF sample with 10^7 dislocations per cm^2. The dislocation density was determined by counting the etch pits on the cleaved surface of the single crystal*. The measurement results have shown that in spite of a dislocation-density difference amounting to four orders of magnitude, the transverse harmonic in the last of these samples was only twice as large.

In view of the very small number of experiments, it is still too early to draw any final conclusions, but it is obvious that cancellation of the positive- and negative-stress microregions (obtained as a result of the fact that the ultrasound reveals the averaged effect) leads to generation of a relatively weak transverse harmonic, smaller than in the case of longitudinal waves.

3. Raman scattering of sound by sound. We have described above experimental methods and results on nonlinear distortion of waves propagating in the same direction. In solids, as already mentioned in Ch. III, unlike in liquids (without dispersion), the so-called Raman scattering of sound by sound, with formation of plane traveling waves of combination frequencies, is possible if the energy and quasimomentum laws are satisfied for plane traveling waves. When these laws or the resonance conditions (20) are satisfied, interactions can occur when the waves intersect at a certain angle. As follows from Table V, such interactions can be quite numerous in the case of three-wave processes.

The Raman scattering of sound by sound was investigated experimentally in a number of studies[68-71].

A block diagram of the setup for the study of such scattering is shown in Fig. 9[71]. Two converters (e.g.,

*For simplicity, we shall henceforth call these positive and negative regions.

*The crystals were prepared by B. A. Reznikov, and the authors take the opportunity to express their gratitude.

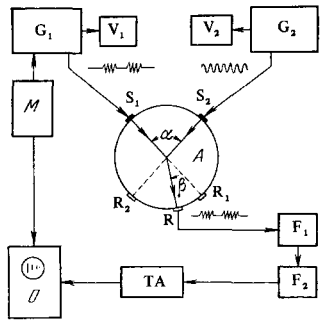

FIG. 9. Block diagram of setup for the investigation of Raman scattering of sound by sound.

quartz plates suitably cut) S_1 and S_2 are excited by an alternating voltage from the generators G_1 and G_2 (V_1 and V_2 are voltmeters). These converters radiate longitudinal or transverse waves of different frequency into the solid-body block A; in[70,71] the measurements were performed in a block of polycrystalline aluminum. These waves intersect, in the form of ultrasonic beams, at an angle α. The combination-frequency wave scattered at the angle β is received further by a receiver R, the resonant frequency of which is equal to the combination frequency. F_1 and F_2 are rejection filters, which block each of the interacting frequencies, TA is an amplifier turned to the combination frequency, O is an indicator, and M is a pulse modulator. The generator G_2 operates in the cw mode and G_1 in the pulsed mode. Naturally, the received scattered signal is pulse-modulated. It is possible to use the pulsed mode also for generator G_2. In this case, however, the pulses from G_1 and G_2 must arrive simultaneously in the interaction region. In Fig. 9, R_1 and R_2 are control receivers. In[71], in the study of the interaction $T(\omega) + T(\omega) = L(2\omega)$ at a frequency 3 MHz, the scattered signal produced voltages on the order of a fraction of a millivolt in the X-cut-quartz controlled resonant receiver when 750 V was applied to the oscillators S_1 and S_2. This amounts to 10^{-3}—10^{-4} of the voltage on one of the control receivers.

Experiments on Raman scattering of sound by sound agree in general with the theory developed in Ch. III. We call attention to the fact that experiments on Raman scattering of sound by sound can be regarded as modulation of nonlinear interactions between thermal phonons or between coherent and thermal phonons, carried out on coherent phonons of relatively low energy.

In the introduction to this article we already indicated that nonlinear interaction between thermal phonons is of great importance in thermal conductivity, and nonlinear interaction between coherent phonons and thermal phonons explains the absorption of sound in dielectric crystals.

As far back as in 1935, on the basis of the assumption of nonlinear interaction between an acoustic wave (coherent phonons) and Debye waves (thermal phonons) resulting from the lattice anharmonicity, L. D. Landau and Yu. B. Rumer[46] developed a theory for the absorption of high-frequency sound in solids (the "LR" theory). According to this theory, the interaction between the coherent and thermal phonons gives rise to a third phonon, and some of the energy of the coherent phonon is transferred to the produced thermal phonon; the sound wave loses energy.

Such direct linear interactions between coherent and thermal phonons can occur, however, only if the length of the sound wave λ_{ac} is much shorter than the mean free path λ_{ph} of the thermal phonon. Only then is a noticeable accumulation of the result of this interaction possible. This defines the condition for the applicability of the "LR" theory, namely $\lambda_{ac} \ll l_{ph}$. Such conditions are satisfied at low temperatures and at hypersonic frequencies. Since $l_{ph} = c\tau_{ph}$, where c is the velocity of the phonon and τ_{ph} the relaxation time (the phonon lifetime), this condition can also be written in the form $\omega\tau_{ph} \gg 1$ (ω—frequency of the sound), since we are considering normal or N-processes and there is no dispersion.

In the proposed three-phonon process it is necessary to satisfy the energy and quasimomentum conditions (20). Since in solids the velocity of the longitudinal waves c_l always exceeds the velocity of the transverse waves c_T, it follows from the conditions (20) and the "LR" theory that in an isotropic medium without dispersion, a low-frequency longitudinal sound wave can interact only with a high-frequency longitudinal wave of thermal origin, and give rise as a result of the interaction to a third longitudinal wave only if all three waves are collinear*. For transverse sound waves, on the other hand, there is no such strong limitation; in this case noncollinear interactions with thermal waves are possible. For this reason, the absorption coefficient α_l for longitudinal waves should be much smaller than the absorption coefficient α_T, for transverse waves. An attempt to explain the phonon absorption of longitudinal waves by taking into account four phonon processes was made in[72]. Experiments have shown later that the contribution of such processes to the absorption of longitudinal waves is, however, not appreciable. As to the dependence of α_T on the frequency ω and on the temperature T, according to "LR" theory we have here $\alpha_T \sim \omega T^4$ if $\lambda_{ac} \ll l_{ph}$†.

The other limiting case $\lambda_{ac} \gg l_{ph}$ was considered by A. I. Akhiezer[73]. In this case there is no direct nonlinear interaction between the coherent and thermal phonons. The acoustic waves change the equilibrium state of the thermal phonons, which then, again as a result of a nonlinear interaction, but now between the thermal phonons themselves, relax anew to their equilibrium state. In[74] an attempt was made to develop a theory covering both the case $\lambda_{ac} \gg l_{ph}$ and the case $\lambda_{ac} \ll l_{ph}$.

The development of the experimental technique of hypersonic measurements, following the work by K. N. Baranskiĭ[60], has made it possible to perform a number of investigations on the absorption of longitudinal and transverse waves in a number of single crystals (quartz, ruby, sapphire, ruby spinel, etc.) at high hypersonic frequencies in a wide range of temperatures—from the temperature of liquid helium to room temperatures[61,75-79]. These investigations have shown that at low temperatures the absorption of both longi-

*Strictly speaking, it is necessary to take into account also other nonforbidden interactions (see Table V). This problem has not yet been theoretically analyzed.

†In many crystals this condition is satisfied at frequencies on the order of several GHz at a temperature close to 10°K.

tudinal and transverse hypersonic waves in high-grade dielectric crystals is very small, and is apparently determined only by the crystal defects (the so-called residual attenuation). With increasing temperature, starting with a temperature close to that of liquid helium, the absorption of the transverse waves increases, and in the region $\omega\tau_{ph} \gg 1$ it agrees in general satisfactorily with the conclusions of the "LR" theory. On the other hand, for the case of longitudinal waves, α_l under these conditions, in contradiction to the conclusions of the "LR" theory, is of the same order of magnitude as α_T, and a similar dependence on ω and T^*.

An attempt to explain the contradiction was made in[82-84]. It was noted that owing to the energy-time uncertainty relation, exact satisfaction of the conservation laws is not essential for the interaction of coherent phonons with thermal ones, in view of the finite relaxation time of these phonons. For this reason, longitudinal sound waves can interact nonlinearly with longitudinal thermal phonons if all three waves are not exactly but only approximately collinear. Allowance for almost-collinear interaction has made it possible to explain qualitatively the absorption of the longitudinal waves. According to these papers, the absorption coefficient of the longitudinal waves, like α_T, is proportional to ωT^4.

To check on the theory of interaction of almost-collinear longitudinal phonons, the following experiment was performed in[85]. Two longitudinal plane waves—one of relatively low frequency (7—50 MHz) and the other of high frequency (200—100 MHz) could propagate in a block of fused quartz in such a way that the angle between the propagation directions of these waves could be varied. At the same time, the condition of the "LR" theory $\omega\tau_{ph} \gg 1$ was satisfied in the experiment, if it is assumed that the high-frequency wave represents a thermal longitudinal phonon, and the low-frequency wave a longitudinal coherent phonon. These experiments were performed at room temperatures using the following procedure (Fig. 10): The low-frequency radiator was secured to a goniometer and

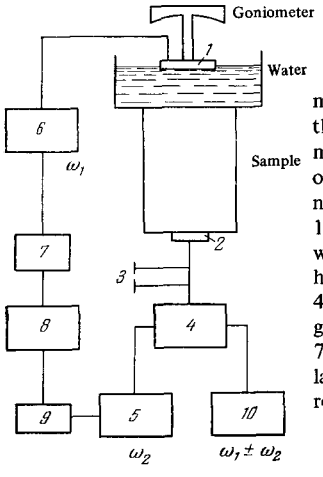

FIG. 10. Block diagram for the measurements of the dependence of the amplitude of the difference or summary frequency of a longitudinal wave on the angle between the two longitudinal waves of low and high frequency. 1—low-frequency X-cut quartz plate with natural frequency $\omega_1 = 7$ MHz, 2—high-frequency radiator ω_2, 3—turning, 4—hybrid junction, 5—high-frequency generator, 6—low-frequency generator, 7—delay line, 8—synchronizer, 9—delay line, 10—combination-frequency receiver.

*A detailed discussion of this entire complicated problem of phonon absorption of sound can be found, for example, in the reviews [80,81].

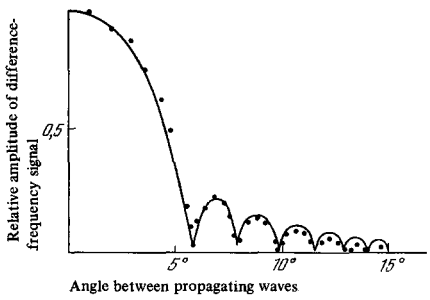

FIG. 11. Angular dependence of the amplitude of the difference frequency in fused quartz. Input frequency 300 and 20.6 MHz. Thick line—theoretical curve, sample—cylinder 5.08 cm long and 2.44 cm in diameter.

could be inclined at a certain angle, being situated in a vessel with water. Part of the low-frequency pulse signal (a pulse method was used) entered the sample. The high-frequency pulse from a converter fastened to the lower part of the sample, was applied at such an instant of time, that after being reflected from the upper surface, the two pulses (of low and high frequency) propagated together and interaction occurred between them. Such an experimental scheme has made it possible to measure the amplitudes of the summary or difference frequencies as functions of the angle between the propagation directions of the longitudinal waves. The theory developed for this case in the cited paper, as seen from Fig. 11, is in sufficiently good agreement with the experiments*.

Thus, the results of[85] agree on the whole with the conclusion that almost-collinear interactions of longitudinal waves can play an important role in the explanation of the absorption of longitudinal waves when the condition $\omega\tau_{ph} \gg 1$ is satisfied.

Summarizing, we can state that experiments on Raman scattering of sound by sound are of appreciable significance when it comes to increasing our knowledge of phonon-phonon interactions.

4. Generation of harmonics in Rayleigh waves. Since the Rayleigh surface wave is localized only in a thin layer near the surface, the elastic-energy density in such a wave, other conditions being equal, is larger than in an exchange wave. The dispersions of Rayleigh waves therefore exhibit no nonlinear phenomena, and harmonic generation[86-88] is strongly manifest in the propagation of these waves.

In[89], the generation of harmonics in a surface wave was investigated in X-cut quartz in the direction of the Y axis. The sample was in the form of a rectangular plate 160 × 60 × 5 mm with Y axis along the large side. A surface wave of fundamental frequency 11 MHz was excited by using a wedge; a voltage up to 200 V was applied to the quartz plate from a 20-W push-pull amplifier. The surface-wave receiver was a variable-phase converter (metal grid), the period of

*We note that qualitatively a similar dependence of the amplitude of the combination frequency should be obtained because the interaction was investigated using bounded sound beams. It is impossible to estimate the periodicity of the oscillations of the combination-frequency amplitude, resulting from the fact that the beams are bounded, since not all the experimental data are quoted in [85].

which corresponded to the length of the surface wave and amounted to 3×10^{-2} cm at the fundamental frequency 11 MHz, and was accordingly half as large at the second-harmonic frequency. The converter-receivers were prepared on a glass plate and could be moved freely over the surface of the quartz. The conversion loss was approximately 40 dB, for the wedge with the quartz plate and 40 and 45 dB for the variable phase converters at 11 and 22 MHz, respectively. A beam of surface waves radiated in the Y direction in the YZ plane was deflected from this axis by 11°, since the direction along the Y axis in the X-cut quartz is not a principal one and the angle between the phase and group velocities for the surface waves propagating in the Y direction amounts to, theoretically, 10°[90].

According to[88], the amplitude of the second harmonic of a Rayleigh wave propagating in α-quartz along the Y axis is determined by the expression $u_x'' = 0.18u_0'^2k^2x$, where u_0' is the amplitude of the fundamental-frequency wave at the radiator and k is its wave number*. The results obtained in[89] for the dependence of the second-harmonic amplitude on the distance between the converter at an angle 11° to the Y axis are shown in Fig. 12. As seen from this figure, the second-harmonic amplitude increases in proportion to the distance and reaches a maximum at $x \approx 10$ cm. Estimates made in the cited paper show that at distances close to the stabilization distance (~ 10 cm), at a maximum acoustic-energy flux density in the surface wave ~ 0.5 W/cm^2, the ratio of the displacement amplitude at the second harmonic to the displacement amplitude at the fundamental frequency is $\sim 0.5\%$.

Just as for volume surface waves, investigations of nonlinear phenomena in the propagation of surface waves are of great importance for the understanding of the mechanism of absorption of these waves. In[91], the damping of Rayleigh waves in a quartz crystal was investigated experimentally at frequencies close to 1 GHz and at low temperatures. It was found that the coefficient of absorption of Rayleigh waves is $\alpha_R \sim \omega T^4$, i.e., it has approximately the same dependence on ω and T as for volume elastic waves. A theoretical analysis of Rayleigh-wave absorption caused by nonlinear interaction of these waves with thermal surface waves, as a result of the anharmonicity of the lattice, was carried out in[92].

5. Nonlinear resonances in acoustic high-Q resonators. It was mentioned in Ch. III that in the case of induced oscillations of nonlinear resonators, if one of the frequencies resulting from the nonlinearity coincides with one of the natural frequencies of the resonator, one can expect the occurrence of certain singularities or "nonlinear resonances."

Figure 13 shows the block diagram for the observation of the detection of a modulated acoustic signal by the nonlinear elasticity of a resonator in the form of a metallic rod[52]. The modulation method of observing nonlinearity in solid samples in the form of rods having a large acoustic Q is very sensitive and makes it possible to observe the nonlinear interaction of elastic waves at sound and ultrasound intensities regarded until recently as the exclusive domain of linear acoustics. In the block diagram, 1 is a high-frequency generator-modulator with high frequency stability. The modulator signal is fed to a high-frequency generator 2. The modulator signal then passes through a rejection filter 3 tuned to the modulation frequency. Beyond this filter, the signal is fed to a piezoelectric converter 5 (X-cut quartz plate) secured to the rod 6. The waves propagating in the rod thus have frequencies corresponding to the components ω and $\omega \pm \Omega$ of the spectrum of the modulated signal. As a result of the nonlinear interaction of these waves with one another, a low-frequency (modulation) wave is separated, i.e., detection is effected by the nonlinear elasticity of the rod. If the modulation frequency coincides with one of the natural frequencies of the rod, resonance takes place. In the block diagram, 7 is a ferromagnetic thin plate glued to the rod (if this rod is not magnetic), 8 is a contactless magnetoelectric receiver, 9 a receiver, 10 an oscillograph, and 4 and 11 voltmeters.

At high Q of the rod, the detected signal is quite large. The amplitude of the acoustically-detected signal depends not only on the equality of the modulation frequency to the natural frequency of the rod, but in the case when the damping of the carrier over the length of the rod is small, it depends also on this carrier frequency. Figure 14 shows a plot of the amplitude of the longitudinal oscillations of the rod at the resonant frequency Ω against the carrier frequency ω[55]. A characteristic triple "resonance" is seen, connected with the fact that there are three frequencies in the spectrum, the carrier and the two side bands; the

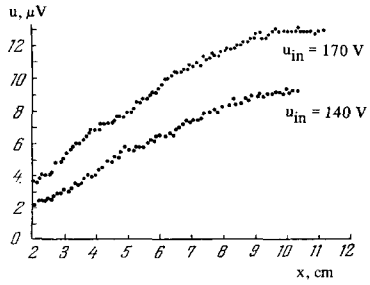

FIG. 12. Dependence of the output voltage of the second harmonic of the Rayleigh wave in a quartz plate (propagation along the Y axis) on the distance between converters. Fundamental frequency 11 MHz.

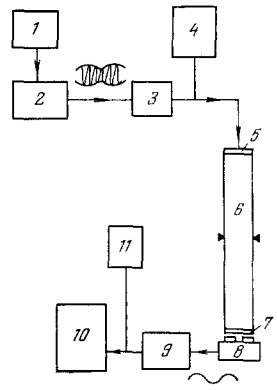

FIG. 13. Block diagram of the modulation method of investigating nonlinear elasticity of solids.

*The numerical coefficient of this formula was obtained in [88] with account taken of known data for the elastic moduli of second and third orders for quartz (see Table II).

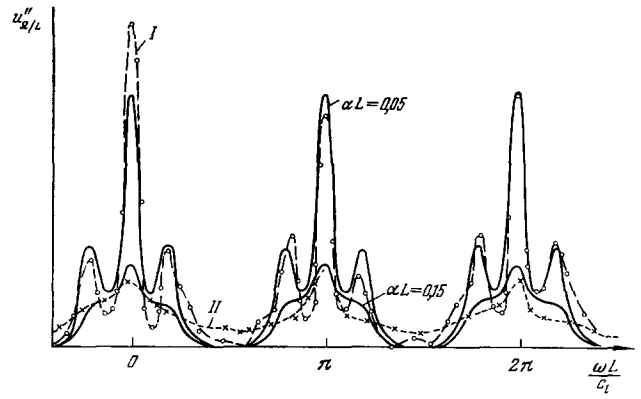

FIG. 14. Amplitude of low-frequency oscillations of aluminum rods excited by modulated oscillations vs. the carrier frequency. Solid curves—in accord with formula (21); the points denote the experimental results for a rod 25 cm long, and the crosses for a rod 75 cm long.

maxima correspond to the condition when the rod resonates not only at the frequency Ω but also at one of the side bands. The same figure shows the calculated curves for the expression in the curly brackets of formula (21). The calculated curves were normalized to one of the maxima of the experimental curves, taken for $\alpha L = 0.05$ and $\alpha L = 0.15$, where α is the attenuation coefficient and L the length of the first and second rods, respectively. The abscissas represent the detuning in units of $\omega L/c_l$ relative to the frequency ω_0, at which $\cos k_l L = 0$. The results presented here correspond to a Reynolds number $Re = u_0 k^2/\alpha \sim 0.05$.

The observation of nonlinear effects at such a small nonlinearity is made possible by the use of a resonance measurement method and by the high Q of the rod ($\sim 10^5$). Similar measurements were made in[53] with transverse waves. It can be assumed that because of its simplicity and high sensitivity, the procedure described above will find use in the investigation of nonlinear acoustic effects.

We note that an experiment similar in principle to that described above was carried out in[93], where an X-cut quartz plate was placed in a microwave resonator. The electromagnetic field excited elastic oscillations in the plate. Owing to the lattice nonlinearity, and in this case also to the nonlinearity of the piezoelectric properties, a constant voltage should be produced across the electrodes of the plate. In this investigation, microwave radiation of 3 GHz was modulated by pulses, and the quartz plate, the Q of which at the carrier frequency was $\sim 6 \times 10^3$, detected the pulses. The detection effect was, naturally, maximal when the carrier frequency coincided with one of the natural frequencies of the piezoelectric plate (at the lowest natural frequency, approximately 20 MHz, this was approximately the 100th overtone of the plate). An estimate given in the cited paper for the contribution of various types of nonlinearities shows that the effect of the nonlinearity of the piezoelectric properties on the detection is smaller by approximately one order of magnitude than the effect of lattice nonlinearity.

6. Optical methods of investigating nonlinear acoustic phenomena. Gas lasers with their large spectral light-flux density have uncovered new possibilities of investigating nonlinear acoustic effects in solids, by using the phenomenon of light diffraction by ultrasonic, and especially hypersonic waves.

The investigation of small nonlinear distortions of an elastic wave by the light-diffraction method encounters, however, a number of difficulties. It might seem that in diffraction by an elastic wave of complicated form it would be possible to estimate the spectrum of the elastic wave from the occurrence of spectra of higher order. This is not the case, however, since in Raman-Nata diffraction, even by a sinusoidal phase grating, spectra of higher order than the first appear. When the diffraction is observed with standard helium-neon lasers, diffraction of the light flux in the spectra of higher order than the first, due to the Raman-Nata diffraction, is larger by at least two orders of magnitude than diffraction of the light flux due to diffraction by acoustic harmonics. Similar difficulties arise also when it comes to separate combination frequencies, unless spatial and temporal selection is effected. In this respect, certain doubts can be cast on the results of[94], where the authors observed the second harmonic at a frequency 21.4 MHz in a NaCl crystal 15 cm long in the Raman-Nata diffraction region.

In[95], nonlinear interaction of two oppositely traveling shear ultrasonic pulses with frequencies 265 and 60 MHz was investigated in fused quartz. According to the synchronism conditions (20), a longitudinal wave should be produced in this case with a frequency equal to the sum of the frequencies of the interacting waves. A pulse of combination frequency was revealed by Bragg diffraction of the beam of a helium-neon laser; the signal was observed by electronic circuitry with storage. The intensity of the interacting waves was several W/cm^2. It was established with the aid of a number of control experiments that the combination-frequency pulse is produced precisely as a result of the nonlinear interaction of two T-pulses.

It should be noted that in the case of Bragg diffraction the difficulties encountered in Raman-Nata diffraction do not arise*. The most thorough work on the optical method of observing harmonics was published in 1968[97]†. The experimental setup is shown in Fig. 15. Light from a stationary helium-neon laser is incident on the investigated transparent crystal, which can be moved along the sound propagation direction, with the Bragg angle θ_B kept constant. This light is diffracted by a longitudinal hypersonic wave (frequencies from 500 MHz upward were used) at an angle θ_B satisfying the Bragg condition $\sin\theta_B = \lambda/2\Lambda$, where λ is the wavelength of the light and Λ the wavelength of the sound. Since the angle θ_B depends on Λ, the harmonics produced by propagation of the hypersonic waves can be investigated independently, by making measurements at angles $\theta_B(\omega)$, $\theta_B(2\omega)$, ...

Such a procedure makes it possible to trace the in-

*We note that a theoretical analysis and an experimental study of Bragg diffraction of light by ultrasound was carried out by S. M. Rytov [96] back in 1937. Although this investigation was carried out for ultrasound propagating in a liquid, its results are applicable to a considerable degree also to Bragg diffraction of light by elastic waves in solids.

†See also [98].

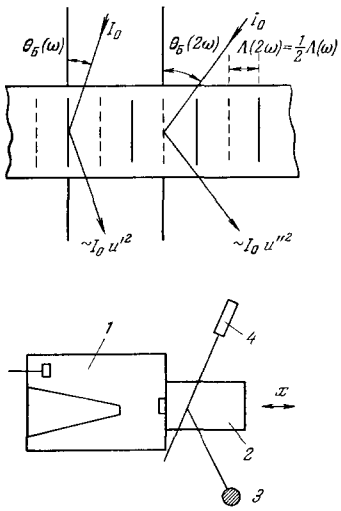

FIG. 15. Diagram of setup for harmonic analysis with the aid of Bragg diffraction. The change of the amplitude of the harmonic with changing distance x is determined by moving the resonator 1 with the crystal 2 relative to the stationary light source 4 and photomultiplier 3.

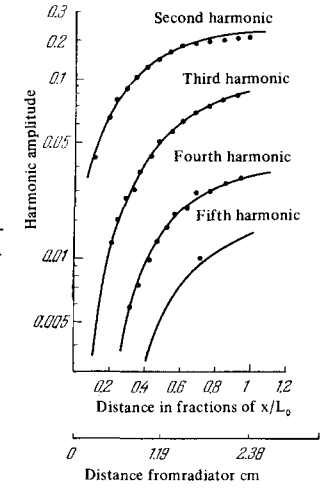

FIG. 16. Harmonic amplitudes (as fractions of the fundamental amplitude) in the propagation of longitudinal waves.

crease and decrease of the harmonics with increasing distance in the crystal, by moving the crystal relative to the laser beam. This is the great advantage of this method over the method of piezoelectric perception of the harmonics, referred to above, although the optical method has its own shortcomings. Another convenience of the method is that at a small ratio of the intensity of the diffracted light to the intensity of the incident light, the intensity of the diffracted light is proportional to the intensity of the sound and is independent of the frequency. This method therefore gives a direct and exact determination of the relative intensity of the harmonic, and many difficulties connected with the calibration of the converters for the absolute measurement of the sound field are eliminated.

The longitudinal waves were radiated by a ZnO plate with lithium admixture and with a resonant frequency 25 MHz. This plate was placed in a coaxial tunable resonator and was excited at the harmonics; the conversion loss was about 10 dB. The pulse duration was 0.5--2.5 μsec, the pulse power (peak) 1—10 W. A helium-neon laser with power 2 MW and light-spot diameter 1 mm was used. The amplitude of the vibrational displacement at 500 MHz was larger by almost two orders of magnitude than in[50,62,63].

Figure 16 shows the distance dependence of the harmonics produced by a 562-MHz longitudinal wave propagating in a quartz crystal along the z axis. The solid lines correspond to the theoretical values obtained under the condition that the distance $L_0 = 2c^2/\beta_l \omega v_0$ at which the break is produced (here c is the velocity of the longitudinal wave, ω is the cyclic frequency, v_0 is the amplitude of the velocity of the first harmonic at the radiator, and β_l is the combination of the nonlinear third-order moduli) equals 2.38 cm and that the absorption coefficient is $\alpha = 0.0866$ cm^{-1}. As seen from the presented experimental data, the second-harmonic amplitude reaches 20% of the fundamental, i.e., the waveform is quite distorted.

Figure 17 shows the results of measurement of the harmonics at 708 MHz for a wave propagating along the z axis of quartz. The abscissas represent the dimensionless distance; the vertical dash-dot line marks the dimension of the crystal. The solid curves

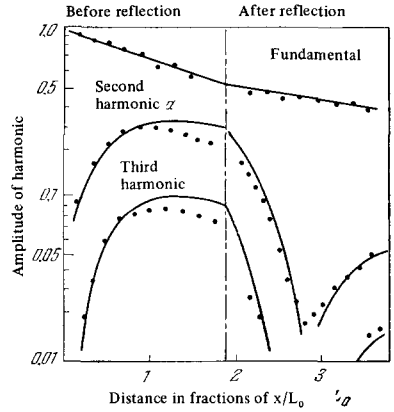

FIG. 17. Behavior of the harmonics of a longitudinal wave.

are theoretical; they are constructed at $L_0 = 1.45$ and $\alpha = 0.138$ cm^{-1}. Here $d/\Lambda = 70$ (d—radius of the rotating plate), and it can be assumed that the measurements are carried out in a plane wave. As seen from Fig. 17, after reflection from the free surface of the crystal, the amplitude of the second harmonic decreases, reaches a minimum, and then again increases, in accord with the fact that when the longitudinal wave is reflected from the free boundary the phase reverses sign.

We have considered above nonlinear wave processes in elastic waves, when these waves were excited with the aid of various electromechanical converters.

The generation of high-frequency hypersound with frequencies on the order of 10^{10} Hz occurs in stimulated Mandel'shtam-Brillouin scattering (SMBS). The scattering of light obtained by focusing a giant laser pulse in a transparent medium, is accompanied by amplification of the elastic (hypersonic) wave from which this scattering takes place[99]. Theoretical estimates and experiment[100,101] show that at room temperatures the intensities of the resultant hypersound are in this case small. Thus, at room temperatures in fused quartz, the maximum power of the hypersound produced in fused quartz with the aid of light from a Q-switched 80-MW/cm^2 laser is 10^{-3} W. Naturally, at such a low hypersound power, the nonlinear phenomena

capable of occurring in this case are small. At the same time, at low helium temperatures, when the absorption of the hypersound in such single crystals as quartz, ruby, sapphire, etc. is very small and the intensities of the hypersound produced in SMBS become appreciable, the nonlinear phenomena can become significant. It is indicated in a number of papers[99,102,103], in particular, that nonlinear acoustic phenomena that lead to the formation of sawtooth waves may be one of the causes of damage to transparent crystals at low temperatures by powerful laser radiation. Apart from indirect data and a number of theoretical estimates, however, there are still no direct measurements of the intensity of hypersound generated in SMBS at low temperatures. There are all the more no experiments on direct observations of harmonic generation in the hypersonic wave of SMBS. So far there is only one experiment[104], in which the appearance of a second harmonic from hypersound of fundamental frequency 5×10^9 Hz was observed in SMBS. In that study, the SMBS was excited by the focused beam of a ruby laser, with power 1–5 MW; the second hypersound harmonic was revealed by scattering the second harmonic of light with λ = 3470 Å, generated with the aid of an ADP crystal, at a Bragg angle 180°.

[1] V. A. Krasil'nikov and A. A. Gedroĭts, Vestnik. MGU, ser. 3, No. 2, 92 (1962).

[2] A. A. Gedroĭts and V. A. Krasil'nikov, Zh. Eksp. Teor. Fiz. 43, 1592 (1962) [Sov. Phys.-JETP 16, 1122 (1963)].

[3] L. K. Zarembo and V. A. Krasil'nikov, Usp. Fiz. Nauk 68, 687 (1958) [Sov. Phys.-Usp. 2, 580 (1960)].

[4] F. Murnaghan, Finite Deformation of an Elastic Solid, New York, John Wiley, 1951.

[5] L. D. Landau and E. M. Lifshitz, Teoriya uprugosti (Theory of Elasticity), Nauka, 1965 [Addison-Wesley].

[6] V. V. Novozhilov, Osnovy nelineĭnoĭ teorii uprugosti (Fundamentals of Nonlinear Theory of Elasticity), M., Gostekhizdat, 1948.

[7] A. E. Green and J. E. Adkins, Large Elastic Deformations and Nonlinear Continuum Mechanics, Oxford, 1960.

[8] D. S. Hughes and J. L. Kelly, Phys. Rev. 92, 1145 (1953).

[9] D. J. Crecraft, Nature 195 (No. 4847), 1193 (1962).

[10] R. T. Smith, Ultrasonics 1, 135 (1963).

[11] S. S. Sekoyan and A. E. Eremeev, Izmeritel'naya tekhnika (Measurement Engineering) No. 7, 25 (1966).

[12] S. S. Sekoyan and A. E. Eremeev ibid. No. 10, 20 (1966).

[13] K. Brugger, Phys. Rev. 133, A1611 (1964).

[14] A. A. Nran'yan, Fiz. Tverd. Tela 6, 2124 (1964) [Sov. Phys.-Solid State 6, 1673 (1965)].

[15] J. H. Parker E. F. Kelly, and D. F. Bolef, Appl. Phys. Lett. 5, 7 (1964).

[16] Z. P. Chang, Phys. Rev. 140, A1788 (1965).

[17] P. B. Gate, Phys. Rev. 139, A1666 (1965).

[18] A. A. Nran'yan, Fiz. Tverd. Tela 5, 177 (1963) [Sov. Phys.-Solid State 5, 129 (1963)].

[19] K. D. Swartz, J. Acoust, Soc. Am. 41, 1083 (1967).

[20] A. L. Stanford and S. P. Zehner, Phys. Rev. 153, $10\bar{2}\bar{5}$ (1967).

[21] J. R. Drubble and R. E. Strathen, Proc. Phys. Soc. 92, 1090 (1967).

[22] M. Gluyas, Brit. J. Appl. Phys. 18, 913 (1967).

[23] T. Bateman, W. P. Mason, and H. J. McSkimin, J. Appl. Phys. 32, 928 (1961).

[24] H. J. McSkimin and P. Andreath, J. Appl. Phys. 35, 3312 (1964).

[25] J. R. Drubble and A. J. Brammer, Proc. Phys. Soc. 91, 959 (1967).

[26] W. B. Gauster and M. A. Breazeal, Naturwiss, Heft 15, 448 (1965).

[27] K. Salama and G. A. Alers, Phys. Rev. 161, 673 (1967).

[28] D. E. Eeastman, J. Appl. Phys. 37, 2312 (1966).

[29] W. B. Gauster and M. A. Breazeal, Phys. Rev. 168, 665 (1968).

[30] D. Gerlich, Phys. Rev. 168, 947 (1968).

[31] E. H. Bogardus, J. Appl. Phys. 36, 2504 (1965).

[32] J. R. Drubble and M. Gluyas, In: Lattice Dynamics, (ed. by R. F. Wallis), Pergamon Press, London, 1965.

[33] Y. Hiki and A. V. Granato, Phys. Rev. 144, 411 (1966).

[34] R. N. Thurston, H. J. McSkimin, and P. Andreath, J. Appl. Phys. 37, 267 (1966).

[35] Z. A. Gol'dberg, Akust, Zh. 4, 307 (1960).

[36] E. Z. Govorova, Nonlinear Interactions of Elastic Waves in Single Crystals, Candidate's dissertation, Moscow Univ., 1966.

[37] M. A. Breazeal and J. Ford, J. Appl. Phys. 36, 3486 (1965).

[38] A. C. Holt and J. Ford, J. Appl. Phys. 38, 42 (1967).

[39] A. L. Polyakova, Fiz. Tverd. Tela 6, 65 (1964) [Sov. Phys.-Solid State 6, 50 (1964)].

[40] A. A. Gedroĭts, L. K. Zarembo and V. A. Krasil'nikov, Dokl. Akad. Nauk SSSR 150, 515 (1963) [Sov. Phys.-Dokl. 8, 478 (1963)].

[41] N. Bloembergen, Nelineĭnaya optika, Benjamin, 1965.

[42] L. K. Zarembo, V. A. Krasil'nikov, and Thai-Than Long, Vestn. MGU, ser. fiz. i astr., No. 5, 132 (1969).

[43] L. K. Zarembo and V. A. Krasil'nikov and Thai-Than Long, ibid. No. 6, 121 (1969).

[44] G. L. Jones and D. R. Kobett, J. Acoust, Soc. Am. 35, 5 (1963).

[45] J. D. Childress and C. G. Hambrick, Phys. Rev. 136, A411 (1964).

[46] L. Landau and G. Rumer, Phys. Zs. Sowjet union 11, 18 (1937).

[47] G. L. Slonimskiĭ, Zh. Eksp. Teor. Fiz. 12, 1457 (1937).

[48] L. N. Taylor and F. R. Rollins, Phys. Rev. 136, A591 (1964).

[49] J. D. Childress and Z. Fried, Bull. Am. Phys. Soc. 8, 16 (1963).

[50] P. H. Carr, Phys. Rev. 169, 719 (1968).

[51] D. H. McMahon, J. Acoust, Soc. Am. 44, 1007 (1968).

[52] L. K. Zarembo, V. A. Krasil'nikov, V. N. Sluch and O. Yu. Sukharevskaya, Akust. Zh. 12, 486 (1966) [Sov. Phys.-Acoust. 12, 421 (1967)].

[53] O. Yu. Sukharevskaya, Vestn. MGU, ser. fiz. i astr. No. 2, 96 (1967).

[54] L. K. Zarembo, Akust, Zh. 16, 58 (1970) [Sov. Phys.-Acoust. 16, 46 (1970)].
[55] L. K. Zarembo and O. Yu. Serdobol'skaya, Vestn. MGU, ser. fiz. i astr. No. 1, 62 (1970).
[56] M. A. Breazeale and D. O. Thompson, J. Appl. Phys. Lett. 3, 77 (1963).
[57] N. S. Shiren, Phys. Rev. Lett. 11, 3 (1963).
[58] P. H. Carr, Phys. Rev. Lett. 13, 332 (1964).
[59] P. H. Carr, IEEE Trans. Sonics Ultrasonics SU-13, 103 (1966).
[60] K. N. Baranskiĭ, Dokl. Akad. Nauk SSSR 114, 517 (1957) [Sov. Phys.-Dokl. 2, 237 (1958)].
[61] H. Bommel and K. Dransfeld, Phys. Rev. 117, 1245 (1960).
[62] K. K. Ermilin, L. K. Zarembo and V. A. Krasil'nikov, Fiz. Tverd. Tela 12, 1329 (1970) [Sov. Phys.-Solid State 12, 1045 (1970).
[63] M. Moriamez, P. Thery, E. Bridoux, and M. Martin, C.r. Acad. Sci. 267 (22), B1195 (1968).
[64] P. Thery, E. Bridoux, F. Haine, and M. Moriamez, C.r. Acad. Sci. 268 (4), B285 (1969).
[65] E. Bridoux, P. Thery, C. Moriamez, and M. Martin, C.r. Acad. Sci. 267 (23), B1260 (1968).
[66] M. Moriamex, E. Bridoux, P. Thery, and F. Haine, C.r. Acad. Sci. 286 (8), B589 (1968).
[67] Akira Hikata, B. B. Chick, and C. Elbaum, J. Appl. Phys. 36, 229 (1965).
[68] F. R. Rollins, Appl. Phys. Lett. 2, 147 (1963).
[69] F. R. Rollins, L. H. Taylor, and P. H. Todd, Phys. Rev. 136, A597 (1964).
[70] Kung Hsin-fan, L. K. Zarembo and V. A. Krasil'nikov, Akust. Zh. 11, 112 (1965) [Sov. Phys.-Acoust. 11, 89 (1965)].
[71] Kung Hsiu-fan, L. K. Zarembo and V. A. Krasil'nikov, Zh. Eksp. Teor. Fiz. 48, 1598 (1965) [Sov. Phys.-JETP 21, 1073 (1965)].
[72] I. J. Pomeranchuk, J. Phys. USSR 6, 237 (1942).
[73] A. Akhieser, J. Phys. USSR 1, 4 277 (1939).
[74] R. O. Woodruff and H. Ehrenreich, Phys. Rev. 123, 1553 (1961).
[75] I. S. Ciccarello and K. Dransfeld, Phys. Rev. 134, A1517 (1964).
[76] E. M. Gonopol'skiĭ and A. N. Chernets, Zh. Eksp. Teor. Fiz. 51, 383 (1966) [Sov. Phys.-JETP 24, 255 (1967)].
[77] M. F. Lewis and E. Patterson, Phys. Rev. 159, 703 (1967).
[78] M. F. Lewis and E. Patterson, J. Appl. Phys. 39, 3420 (1968).
[79] M. Pomerantz, Phys. Rev. 139, A501 (1965).
[80] P. Clemens, in: Physical Acoustics (W. Mason, ed.), V. 3, part B, Chap. 5, Academic Press, 1965.
[81] W. Mason, Ibid., chap. 6.
[82] S. Simons, Proc. Phys. Soc. (London) 82, 401 (1963).
[83] A. J. Maris, Nature 198, 876 (1963).
[84] A. J. Maris, Phil. Mag. 9, 901 (1964).
[85] H. H. Barrett and J. H. Matsinger, Phys. Rev. 154, 877 (1967).
[86] F. Rischbieter, Acoustics 16, 75 (1965/1966).
[87] F. Rischbieter, Acoustics 18, 109 (1967).
[88] P. O. Lopen, J. Appl. Phys. 39, 5400 (1968).
[89] V. A. Krasil'nikov, V. E. Lyamov and I. Yu. Solodov, Vestn. MGU, ser. fiz. i astr., No. 4, 470 (1970).
[90] G. A. Coquin and H. F. Tiersten, JASA 41 (part 2), 921 (1967).
[91] E. Salzman, T. Plieninger, and K. Dransfeld, Appl. Phys. Lett. 13, No. 1, 14 (1968).
[92] A. A. Maradudin and D. L. Mills, Phys. Rev. 177, 881 (1968).
[93] P. H. Carr and A. J. Slobodnik, J. Appl. Phys. 38, 5153 (1967).
[94] J. H. Parker, E. F. Kelly, and D. I. Bolef, Appl. Phys. Lett. 5, 7 (1969).
[95] R. W. Dixon, Appl. Phys. Lett. 11, 340 (1967).
[96] S. M. Rytov, Izv. Akad. Nauk SSSR, ser. fiz. No. 2, 223 (1937).
[97] B. A. Richardson, R. B. Thompson, and C. D. W. Wilkinson, J. Acoust. Soc. Am. 44, 1608 (1968).
[98] M. G. Cohen, IEEE J. Quantum Electronics QE-6 (1), 25 (1970).
[99] V. S. Starunov and I. L. Fabelinskiĭ, Usp. Fiz. Nauk 98 (3), 441 (1969) [Sov. Phys.-Usp. 12, 463 (1970)].
[100] C. L. Tang, J. Appl. Phys. 37, 2945 (1966).
[101] J. Walder and C. L. Tang, Phys. Rev. Lett., 19, 623 (1967).
[102] A. L. Polyakova, ZhETF Pis. Red. 4, 132 (1966) [JETP Lett. 4, 90 (1966)].
[103] A. L. Polyakova, ZhETF Pis. Red. 7, 76 (1968) [JETP Lett. 7, 57 (1968)].
[104] R. G. Brewer, Appl. Phys. Lett. 6, 165 (1965).

Translated by J. G. Adashko